New insight on rheology of self-consolidating earth concrete (SCEC)

Mojtaba Kohandelnia, Masoud Hosseinpoor, Ammar Yahia, Rafik Belarbi

New insight on rheology of self-consolidating earth concrete (SCEC)

Mojtaba Kohandelnia[a,b,*], Masoud Hosseinpoor[a], Ammar Yahia[a], and Rafik Belarbi[a,b,c]

[a]*Université de Sherbrooke, Department of Civil and Building Engineering, Sherbrooke, Québec, Canada*

[b]*La Rochelle Université, LaSIE UMR CNRS 7356, La Rochelle, France*

[c]*Canadian University Dubai, Department of Architecture, City Walk Dubai, United Arab Emirates*

[*]*Corresponding author: Mojtaba.Kohandelnia@usherbrooke.ca*

Abstract

Self-consolidating earth concrete (SCEC) is a novel alternative to facilitate the earth-based construction. A new concrete-equivalent mortar (CEM) approach with constant excess-paste (EP) thickness was proposed to evaluate the rheological and thixotropic properties of various SCEC mixtures proportioned with different clay and superplasticizer types. The use of non-esterified polycarboxylate (NE-PC) and sodium polynaphtalene superplasticizer types in combination with a finer clay type led to a thixotropic behavior. Mixtures made with sodium hexametaphosphate resulted in significantly high yield stress and plastic viscosity values. The rheological properties were mainly controlled by the admixture type, followed by the type and content of clay and water-to-powder ratio (W/P). Empirical models were proposed to predict the rheology of earth-based paste, CEM, and SCEC mixtures using the governing key mixture parameters, including the fineness of the powder constituents (i.e., clay, silt, and cement), water content, EP thickness, paste volume, and packing of the granular skeleton.

Keywords: Clay; Concrete-equivalent mortar; Rheology; Self-consolidating earth concrete; Thixotropy.

1. Introduction

Earth construction goes back to 100 centuries ago and is still used worldwide under different climate conditions [1]. This technique includes cob, mud and adobe masonry bricks, and rammed-earth construction. Environmental-friendly earth construction can be a solution to address the global climate-change concern, because of their availability, durability, economic, and thermal comfort [2,3]. Cement-stabilized earth or soil, mostly used for wall applications, is widely used as layer-by-layer casting and renowned as rammed-earth (RE) with favorable performance [4]. However, RE construction process is time consuming because of the mechanical consolidation to achieve targeted performance and induces deficiencies due to its layer-by-layer nature [5]. Self-consolidating earth concrete (SCEC) can be an alternative to address these abovementioned defects while preserving the advantages of RE technique.

Self-consolidating concrete (SCC) is typically proportioned with relatively higher volume of paste (V_P) than conventional concrete to improve workability. Supplementary cementitious materials (SCM) are therefore used to partially replace cement and reduce the clinker factor of SCC. In the case of SCEC, the binder system consists generally in a ternary mixture of very fine clay and silt particles contained in earth, in addition to cement [6–9]. Different test measurements are employed to identify the key characteristics of clay and silt constituents of the binder that can be used to classify soils and assess their suitability given the application on hand. The Atterberg limits of soil are highly influenced by the type and content of clay, hence they can be useful in classifying soil behaviors in presence of water [10–13].

Suspensions containing high volumetric content of fine particles generally exhibit high yield stress and plastic viscosity values due to high interparticle frictions [14–16]. The use of high-range water-reducer (HRWR) is therefore necessary to achieve good deformability of SCEC mixtures containing fine clay particles. Good compatibility between the HRWR and ternary binder system in SCEC matrix is essential to ensure proper dispersion of fine particles [6] and achieve adequate workability. The efficiency of polycarboxylate-ether (PCE) based superplasticizers on ternary binder system of SCEC has been reported in literature [9]. On the other hand, inorganic dispersing agents, such as sodium hexametaphosphate (NaHMP), were also found very effective to disperse clay particles by electrostatic repulsion forces [17–19]. Therefore, evaluating rheology of SCEC mixtures proportioned with different types and content of clay, as well admixture types can be of interest to achieve adapted rheology given the application on hand.

Structural build-up of the cementitious materials can be evaluated by various rheometric measures including: (1) the evolution rate of the static yield stress [20–22], (2) storage (G′) and loss (G″) moduli over time [21,23], and (3) the area enclosed between the ascending and descending flow curves (i.e., the hysteresis loop). The latter refers to the rebuilding energy at various time intervals and has been frequently used in literature as an indication of structuration kinetics [24,25]. The selection of the geometry is also critical to limit wall slip and liquid phase migration risks [26,27]. Using coaxial geometry limits the maximum aggregate size, while the results of parallel-plates rheometry is questionable due to the evaporation and wall-slip risk [28,29]. However, regarding the shortcomings of coaxial geometry, using parallel-plates set-up can be more favorable to measure the rheological properties of earth-based suspensions due to the presence of silt particles (up to 75 μm). The rheological measurements are affected by various physicochemical synergies, including flocculation of the binder particles and nucleation of hydration products. The binder compositions, solid concentration, existence of colloidal particles, as well as the type and dosage of admixtures are key influencing factors [21]. In the case of mortar and concrete mixtures, the volumetric content and particle-size distribution (PSD) of aggregate can significantly affect the rheological measurements [30], reflected by the viscoplastic properties, including yield stress and plastic viscosity. The evaluation of static yield stress of cementitious materials is challenging due to the effect of the adopted testing protocol, shear history, elapsed time, and ambient conditions [31]. In the case of ternary binder system of SCEC, the applied shear protocol is even more important due to the risk of liquid-phase migration [32].

The concrete equivalent mortar (CEM) approach has been widely used to predict the performance of its corresponding concrete. The CEM mixtures are proportioned to achieve the same surface area of coarse and fine aggregate existing in its corresponding concrete mixture [33]. The CEM approach was widely used to simulate different properties of concrete in fresh and hardened states. This approach was successfully used to simulate the interaction between the binders and admixtures, and evaluate the robustness of the workability and rheological properties of SCC mixtures [34]. Strong relationships were established between the fresh and hardened properties of CEM and concrete [33,35,36]. The established correlations can facilitate the optimization process and reduce the number of trial batches and materials. Although the surface area of aggregate is maintained constant in the conventional CEM approach, the excess paste (EP) thickness can change due to packing density of coarse and fine aggregate [7]. This can therefore negatively affect the accuracy of the conventional CEM to reproduce the workability and rheology of concrete mixtures. The EP concept was also introduced to improve the accuracy of CEM to predict the properties of concrete [37,38]. The CEM approach can be beneficial to be considered from two different perspectives, including (i) applicability of this approach to control the performance of SCEC and (ii) rheology of each CEM mixture which itself can be considered as an independent self-consolidating earth mortar, since earth particles are commonly consisted in finer particles compared to conventional concrete.

In this context, the CEM approach considering the constant EP thickness is used in this study. Accordingly, the coupled effect of binder constituents, including type and content of clay, cement content, water-to-powder ratio, paste volume, EP thickness, volumetric sand-to-total aggregate ratio, and admixture type on rheology and thixotropy of paste, CEM, and SCEC mixtures is investigated using the proposed CEM approach. The significance of key parameters affecting the rheological behavior of multiscale self-consolidating earthen-cementitious suspensions was highlighted. Due to the diversity of soil types used, plasticity index (PI) was used as their representative parameter which is highly dependent on the presence of fine particles. Various empirical models were established to predict the rheological behavior of self-consolidating earth-based paste mixtures from their workability parameters. Subsequently, the rheological properties of the CEM and SCEC mixtures were predicted as functions of the characteristics of their corresponding paste and CEM mixtures, respectively.

2. Methodology

2.1. Materials and testing methods

Two different clay types were used, including a pure kaolinite with specific surface area (SSA) of 15 m^2/g and specific gravity of 2.73 (Type I), and a combination of 50% kaolinite and 50% attapulgite (wt.% by mass) having SSA of 155 m^2/g and specific gravity of 2.75 (Type II). A general use Portland cement (GU) and quartz silt powder (2 to 75 µm) with specific gravities of 3.15 and 2.69, respectively, were used. Two common inorganic dispersant agents in clay industry were used, including high purity sodium hexametaphosphate (NaHMP) with solid ratio of 37.1% and sodium silicate solution (NaSil) with 10.6% Na_2O, 26.5% SiO_2, and 72.9% H_2O (wt.% by mass). Three commonly used HRWR types in concrete industry, including polycarboxylate ether (PCE), sodium polynaphtalene (PNS), and non-esterified polycarboxylate (NE-PC) were also employed. The aggregate used to proportion the investigated SCEC mixtures included natural river sand (0-5 mm) and crushed limestone gravel (5-10 mm) with specific gravities of 2.67 and 2.72 and water absorptions of 1.09% and 0.42%, respectively. The PSDs of the aggregate are presented in Fig. 1.

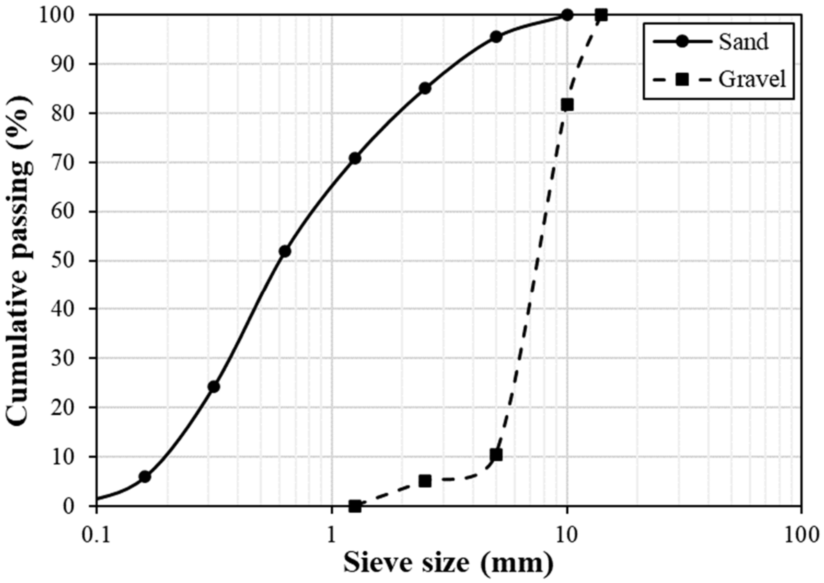

Fig. 1. Particle-size distributions of the sand and gravel.

The rheological behavior of the SCEC mixtures was investigated using the novel concrete-equivalent mortar (CEM) approach proposed by Kohandelnia et al. [7]. As mentioned earlier, in the case of conventional CEM method, only the total surface area of aggregate is constant [35,37], while the change in packing density of granular skeleton in concrete (sand and gravel) to that of sand in the equivalent mortar was neglected. As can be observed in Fig. 2, for a unit volume of concrete, only a given paste volume, namely compacted volume of paste (V_{CP}), is required to fill the voids between the compacted aggregate (V_{CA}), knowing that the volumetric fraction of aggregates (φ) in concrete is lower than its packing density (φ_{max}). The remaining paste, referred to the excess volume of paste (V_{EP}), contributes to improving the flowability of the mixture by reducing the inter-particles friction. The excess volume of paste ($V_{EP} = 1- \frac{\varphi}{\varphi_{max}}$) can be calculated using the ratio of the volumetric content of aggregates-to-their packing density ($\frac{\varphi}{\varphi_{max}}$), namely relative-solid packing fraction [39]. The required sand content to proportion the new proposed CEM mixture with similar excess paste thickness (e_{EP}) to that of its corresponding concrete mixture can be calculated as follow:

$$e_{EP\text{-}CEM} = e_{EP\text{-}Concrete} \Rightarrow \frac{V_{EP\text{-}CEM}}{A_{eq:\,sand}} = \frac{V_{EP\text{-}Concrete}}{A_{sand+gravel}} \Rightarrow \frac{1 - \frac{\varphi_{eq:sand}}{\varphi_{max:sand}}}{A_{eq:sand}} = \frac{1 - \frac{\varphi_{sand+gravel}}{\varphi_{max:sand+gravel}}}{A_{sand+gravel}} \quad (1)$$

where $V_{EP\text{-}Concrete}$, $V_{EP\text{-}CEM}$, $\varphi_{sand+gravel}$, $\varphi_{eq:sand}$, $\varphi_{max:sand+gravel}$, $\varphi_{max:sand}$, $A_{sand+gravel}$, and $A_{eq:sand}$ are the excess volume of paste, volumetric content, packing density, and surface area of aggregate in SCEC (sand and gravel) and its corresponding CEM mixture (sand), respectively. In order to ensure higher accuracy of the aggregate' morphology, the 3D surface area-to-volume ratio (A_{3D}/V) of sand and gravel particles was evaluated using Max3D laser scanner and X-ray micro-CT scanner for different aggregate subclasses of sand and gravel, corresponding to the standard sieves, larger and smaller than 1.25 mm, respectively. According to the image analyses results, the A_{3D}/V ratios of 21583.4 and 859.8 m^2/m^3 (as summarized in Table 1A in the Appendix) were obtained for the sand and gravel particles used in this study, respectively.

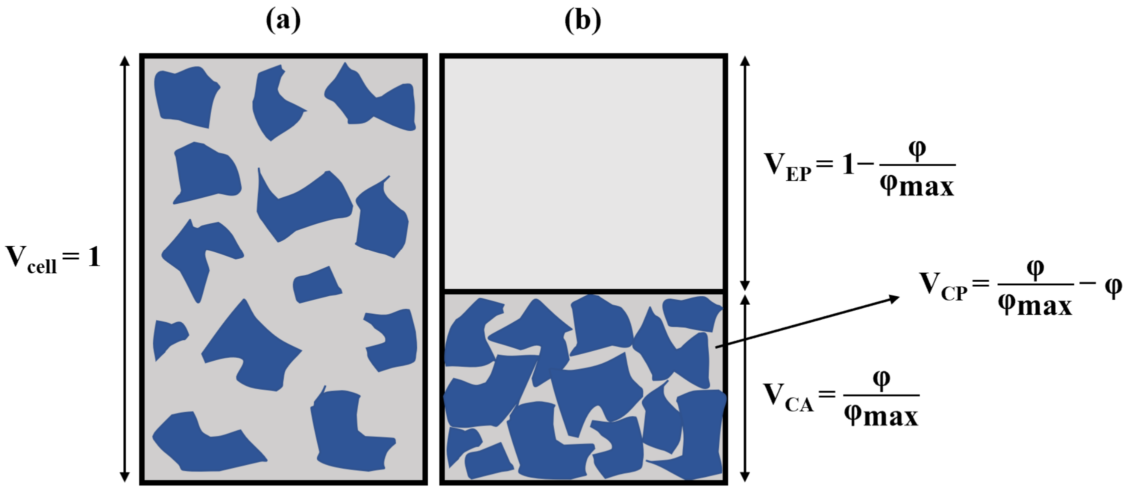

Fig. 2. (a) Schematic of a unit volume of concrete ($V_{cell} = 1$) as a suspension of sand and gravel particles in paste, (b) excess volume of paste (V_{EP}), compacted aggregate (V_{CA}), and compacted paste volume (V_{CP}).

The paste and mortar mixtures were prepared using a planetary Hobart mixer conforming to the ASTM C305 specifications [40]. The mini-slump flow (MSF) [41] of paste and CEM mixtures was assessed at 0, 30, and 60 min after mixing. Mini-V-funnel (MVF) [42] and marsh cone (MCT) [43] tests were also employed to evaluate the flowability of the investigated mortar and paste mixtures, respectively. Workability of concrete mixtures were evaluated using the slump flow (SF) [42] and V-Funnel [44] tests. The Atterberg limit tests, including the liquid limit (LL), plastic limit (PL), and plasticity index (PI = LL - PL), were carried out according to the ASTM D4318 specifications [45] to characterize the soil (i.e., clay, silt, and sand < 425 µm). Rheometric tests were conducted on the investigated paste mixtures using the Anton Paar MCR 302 rheometer with parallel-plates geometry, as shown in Fig. 3. It should be noted that coaxial geometry could not be employed due to the presence of silt particles up to 75 µm. The viscoplastic properties of the paste mixtures were measured using a shearing protocol that consists in applying a pre-shearing of 150 s^{-1} for 120 s, followed by stepwise descending regime to a shear rate of 1 s^{-1} during 105 s, as shown in Fig. 4a.

Moreover, a hysteresis-loop shearing protocol was applied to evaluate the thixotropy of the paste mixtures, as shown in Fig. 4b. This consists in applying a pre-shearing of 50 s^{-1} for 30 s, followed by a 30-s resting period (0 s^{-1}). After the resting period, the shear rate values increased step-wise from 0.1 s^{-1} to 150 s^{-1} during 90 s, followed by a step-wise shear-rate reduction to its initial value 0.1 s^{-1} for another 90-s period [46–48]. The enclosed area between the increasing (Up) and decreasing (Down) shear stress-shear rate curves was then calculated and used to assess the breakdown and thixotropy of the investigated paste mixtures, described as A_{thix} [49]. On the other hand, the ConTec 5 and 6 viscometers were used to evaluate the rheological properties of the investigated concrete mixtures and their corresponding CEMs, respectively.

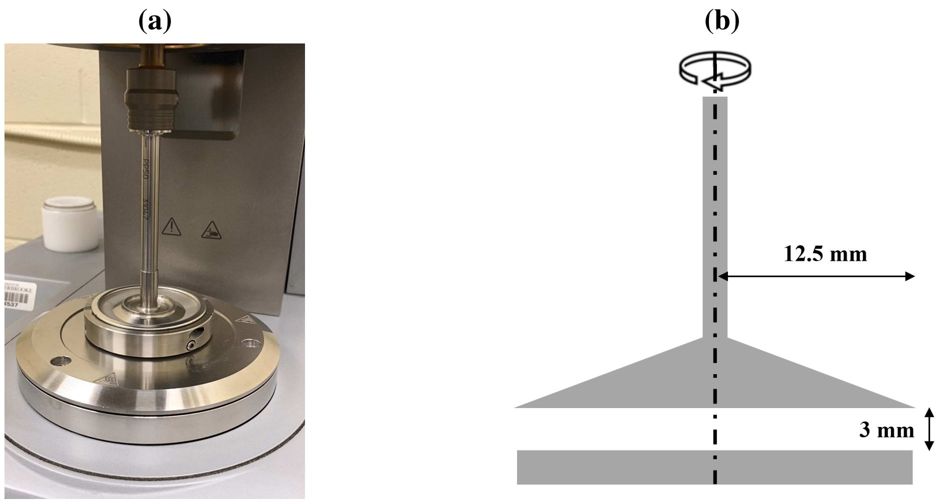

Fig. 3. (a) AntonPaar MCR302 rheometer with parallel-plate geometry and (b) schematics of the parallel-plates set-up.

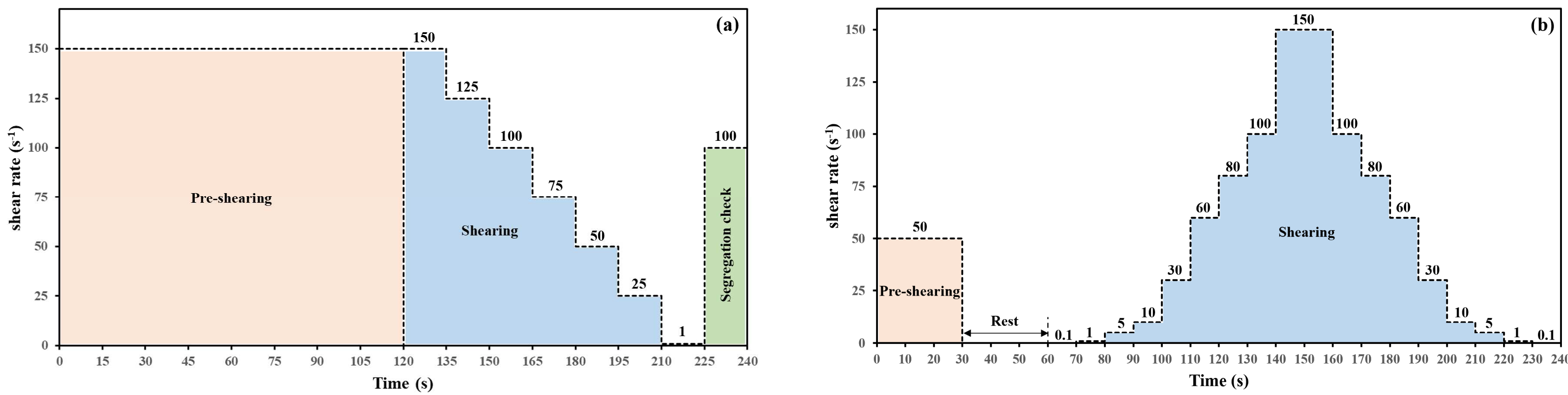

Fig. 4. Shear protocol employed to assess (a) viscoplastic properties and (b) thixotropy of the investigated paste mixtures.

The Bingham and Herschel-Bulkley models were applied to estimate the rheological parameters of the investigated mixtures, as follow:

$$\text{Bingham model: } \tau = \tau_0 + \mu_p \times \dot{\gamma} \quad (2)$$

$$\text{Herschel-Bulkley model: } \tau = \tau_0 + k \times \dot{\gamma}^n \quad (3)$$

where τ, τ_0, μ_p, $\dot{\gamma}$, k, and n are shear stress, yield stress, plastic viscosity, shear rate, consistency, and pseudoplastic indices, respectively. A pseudoplastic index "n" value lower than 1 corresponds to a shear-thinning behavior, identified by a decrease in the apparent viscosity under higher shear rates, which is typical for conventional cement-based materials. On the other hand, the "n" value greater than 1 corresponds to a shear-thickening behavior, reflected by an increase in the apparent viscosity values under higher shear rates. It must be also noted that the viscoplastic and thixotropic measurements were carried out at 0, 30, and 60 min after mixing.

2.2. Mixtures proportioning

As summarized in Table 1, five different cement contents, paste volumes (V_P), water-to-powder (W/P), cement-to-clay (Ce/Cl, by mass), and volumetric sand-to-total aggregate (S/A) ratios, and five different types of admixtures were investigated in this study. Moreover, two clay types with highly different fineness were selected to cover a wide range of soil types. As can be observed in Table 1, the investigated V_P values are relatively higher than those in conventional SCC mixtures to simulate the presence of ternary binder system existing in earth concrete (i.e., clay, cement, and silt). Moreover, wide ranges of W/P (0.30 to 0.50) and Ce/Cl (0.50 to 1.50) were investigated. Furthermore, different S/A of 0.5 to 0.9 were selected to investigate the effect of aggregate packing on rheological properties of the investigated SCEC mixtures. The synergy of the binders used in combination with two inorganic dispersants and three common superplasticizers on rheology of the investigated mixtures was studied. Based on the Taguchi orthogonal array L_{50} ($2^1 \times 5^6$), 50 experiments were conducted to evaluate the coupled effect of the abovementioned factors on rheological behavior of the investigated SCEC mixtures.

Table 1. Investigated parameters and their corresponding levels to proportion the investigated SCEC mixtures [6].

Levels	Factors						
	Clay type	Cement content (kg/m^3)	V_P (%)	W/P	Ce/Cl	S/A	Admixture type
1	Type I	60	45	0.30	0.50	0.5	NaHMP
2	Type II	90	48	0.35	0.75	0.6	NaSil
3	-	120	51	0.40	1.00	0.7	PCE
4	-	150	54	0.45	1.25	0.8	PNS
5	-	180	57	0.50	1.50	0.9	NE-PC

First, 18 paste mixtures were selected out of the 50 investigated mixtures [6] to proportion the CEM mixtures, based on their 1-day compressive strength (> 1 MPa) and admixture demand to achieve a targeted MSF of 280 ± 20 mm. Similarly, the MSF values of the 18 selected CEM mixtures were assessed to secure the targeted MSF of 280 ± 20 mm. Finally, according to the CEM results, three SCEC mixtures were selected. It is worthy to mention that only the SCEC mixtures proportioned with PCE were chosen as the optimum admixture type effect [7]. Moreover, a reference concrete mixture (C_{ref}) and its corresponding CEM (M_{ref}) were also investigated. These mixtures were proportioned with PCE, but without any clay content. The mixture proportioning of the investigated paste (P), CEM (M), and SCEC (C) mixtures are summarized in Table 2.

Table 2. Proportioning of the investigated paste, CEM, and SCEC mixtures [7].

	Mix No.	Admixture type	Cement (kg/m^3)	Water (kg/m^3)	Clay (kg/m^3)		Silt (kg/m^3)	W/P	V_P (%)	Sand (kg/m^3)	Gravel (kg/m^3)	S/A	e_{EP} (μm)
					Type I	Type II							
Paste	P6	NE-PC	200.0	490.7	173.3	-	1028.5	0.35	-	-	-	-	-
	P10	PNS	157.9	450.9	182.5	-	1162.5	0.30	-	-	-	-	-
	P11	PNS	266.7	526.2	154.1	-	894.9	0.40	-	-	-	-	-
	P12	NE-PC	250.0	556.3	433.3	-	553.0	0.45	-	-	-	-	-
	P15	PCE	210.5	490.9	146.0	-	1046.0	0.35	-	-	-	-	-
	P16	PCE	333.3	558.7	385.2	-	523.0	0.45	-	-	-	-	-
	P17	PNS	312.5	584.1	270.8	-	584.9	0.50	-	-	-	-	-
	P18	NE-PC	294.1	454.2	203.9	-	1016.0	0.30	-	-	-	-	-
	P22	PCE	375.0	456.2	216.7	-	929.1	0.30	-	-	-	-	-
	P23	PNS	352.9	495.8	611.8	-	452.0	0.35	-	-	-	-	-
	P24	NE-PC	333.3	528.8	385.2	-	603.4	0.40	-	-	-	-	-
	P25	NaHMP	315.8	557.8	273.7	-	650.1	0.45	-	-	-	-	-
	P26	PNS	133.3	450.1	-	92.4	1274.4	0.30	-	-	-	-	-
	P32	PNS	187.5	524.2	-	216.7	906.3	0.40	-	-	-	-	-
	P37	PCE	250.0	555.6	-	173.3	811.3	0.45	-	-	-	-	-
	P44	PNS	277.8	492.9	-	240.7	889.7	0.35	-	-	-	-	-
	P45	NE-PC	263.2	526.2	-	182.5	869.9	0.40	-	-	-	-	-
	P49	PCE	333.3	528.2	-	192.6	794.6	0.40	-	-	-	-	-
CEM	M6	NE-PC	100.0	245.3	86.7	-	514.2	0.35	45	1197.2	-	1	40.2
	M10	PNS	101.6	290.1	117.4	-	748.0	0.30	57	815.6	-	1	88.4
	M11	PNS	149.3	294.6	86.2	-	500.9	0.40	45	1038.0	-	1	56.0
	M12	NE-PC	139.6	310.7	242.0	-	308.8	0.45	48	1041.6	-	1	55.6
	M15	PCE	147.0	342.8	101.9	-	730.4	0.35	57	669.6	-	1	121.4
	M16	PCE	157.7	264.3	182.2	-	247.4	0.45	45	1268.7	-	1	34.4
	M17	PNS	192.8	360.4	167.1	-	360.9	0.50	48	885.6	-	1	76.5
	M18	NE-PC	181.5	280.4	125.9	-	627.2	0.30	51	885.1	-	1	76.5
	M22	PCE	198.7	241.7	114.8	-	492.2	0.30	48	1117.7	-	1	47.6
	M23	PNS	188.1	264.3	326.1	-	240.9	0.35	51	1109.1	-	1	48.4
	M24	NE-PC	224.1	355.5	259.0	-	405.7	0.40	54	738.4	-	1	104.2
	M25	NaHMP	212.0	374.5	183.7	-	436.4	0.45	57	741.4	-	1	103.5
	M26	PNS	63.1	212.9	-	43.7	602.9	0.30	45	1268.7	-	1	34.4
	M32	PNS	99.3	277.7	-	114.8	480.2	0.40	48	1117.7	-	1	47.6
	M37	PCE	147.2	327.2	-	102.1	477.8	0.45	48	960.3	-	1	65.6
	M44	PNS	179.1	317.8	-	155.2	573.6	0.35	54	812.1	-	1	89.1
	M45	NE-PC	169.3	338.6	-	117.4	559.7	0.40	57	815.6	-	1	88.4
	M49	PCE	187.6	297.3	-	108.4	447.2	0.40	54	1030.1	-	1	56.9
	M_{ref}	PCE	818.7	327.5	-	-	-	0.40	45	964.5	-	1	65.1
SCEC	C16	PCE	150.0	251.4	173.3	-	235.3	0.45	45	1197.0	136.0	0.9	34.4
	C22	PCE	180.0	219.0	104.0	-	445.9	0.30	48	1000.2	255.7	0.8	47.6
	C37	PCE	120.0	266.7	-	83.2	389.4	0.45	48	750.1	511.4	0.6	65.6
	C_{ref}	PCE	627.2	250.9	-	-	-	0.40	45	665.0	680.0	0.5	65.1

3. Results and discussion

3.1. Rheology of paste mixtures

The Atterberg limits of the investigated soils (clay, silt, and sand < 425 μm) and thixotropy indices of their corresponding paste mixtures are summarized in Table 3. The Atterberg limits were used as an indication of the binder contribution on soil behavior. Wide ranges of LL (15.7%–36.5%), PL (14.5%–23.6%), and PI (1.2%–13.3%) ensured a comprehensive investigation of various earth types. On the other hand, the evolution rate of the static yield stress, reflecting the thixotropic response, was used to assess the kinetics of structuration [21,22]. For instance, the hysteresis loops of the mixtures P44 and P49, determined immediately after mixing (i.e., t = 0), are illustrated in Fig. 5a and 5b, respectively. As can be observed, in the case of P44, the descending shear stress values were lower than the ascending ones, hence reflecting a thixotropic behavior. However, in the case of P49, a rheopectic behavior, reflected by higher descending shear stresses compared to the ascending ones, was observed. The enclosed area between the upward and downward steps was calculated for all the investigated mixtures. It should be noted that positive and negative values refer to thixotropic and rheopectic behaviors, respectively.

Table 3. Atterberg limits of the earths used (clay, silt, and sand < 425 µm) and thixotropy indices of the investigated paste mixtures.

Mix No.	Clay type	Admixture type	Atterberg limits			A_{thix} (Pa/s)		
			LL (%)	PL (%)	PI (%)	0 min	30 min	60 min
P6	Type I	NE-PC	15.7	14.5	1.2	153	242	151
P10		PNS	18.6	16.9	1.7	-47	-96	-674
P11		PNS	18.1	16.6	1.5	-371	-501	-607
P12		NE-PC	20.1	14.6	5.5	174	200	176
P15		PCE	17.5	16.2	1.3	-145	-117	-77
P16		PCE	18.9	14.9	4	-100	-109	-90
P17		PNS	19.5	15.7	3.8	-602	-642	-711
P18		NE-PC	19.9	16.3	3.6	214	112	120
P22		PCE	18.9	15.8	3.1	223	241	272
P23		PNS	21.5	14.8	6.7	-76	-118	-109
P24		NE-PC	21.6	14.5	7.1	101	78	68
P25		NaHMP	20.5	15.6	4.9	-1138	-1003	-1517
P26	Type II	PNS	21.5	18.3	3.2	636	710	1296
P32		PNS	30.8	23.6	7.2	182	-242	-2375
P37		PCE	32.8	21.8	11	-1628	-1664	-1967
P44		PNS	36.5	23.2	13.3	1123	1322	1413
P45		NE-PC	34.6	22.8	11.8	604	469	440
P49		PCE	31.5	20.5	11	-2629	-2695	-2740

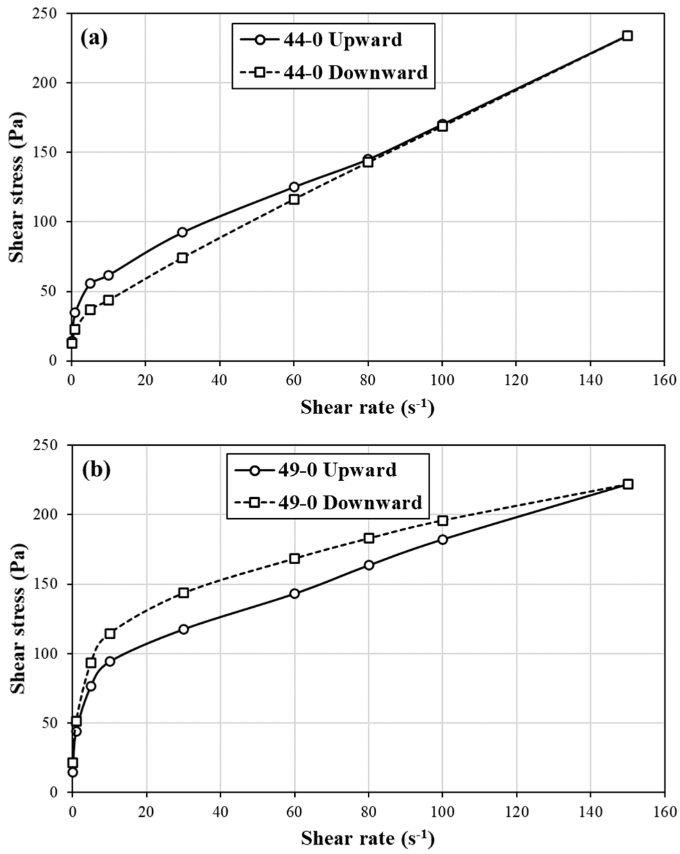

Fig. 5. The hysteresis loops observed for (a) P44 (thixotropy) and (b) P49 (rheopexy) paste mixtures at t = 0.

According to the A_{thix} values obtained immediately after mixing (t = 0) and summarized in Table 3, the thixotropic and rheopectic behaviors of the investigated mixtures were mostly affected by the admixture type. Accordingly, all the NE-PC-based mixtures showed a thixotropic behavior ($A_{thix} > 0$). Moreover, in addition to the mixture P22, proportioned with the lowest W/P and PCE admixture, all the mixtures proportioned with PNS admixture and Clay Type II also exhibited a thixotropic behavior. The mixture P44, containing the highest content of Clay Type II, showed the highest thixotropy response, while the highest rheopectic response was observed for the P49 mixture followed by the P37 and P25 mixtures. In fact, the P49 and P37 paste mixtures made with PCE and Clay Type II, while the mixture P25 was the only system dispersed with NaHMP. Furthermore, the Clay Type II having higher Atterberg limits exhibited greater magnitude of thixotropic/rheopectic response. It is worth mentioning that the behavior of P32 changed over time from thixotropic to highly rheopectic. This mixture was proportioned with the highest W/P among the thixotropic PNS-based mixtures. This suggests that the type of admixture and its synergy with clay type had a dominant effect on the structuration of earth-based paste mixtures, followed by W/P.

The thixotropy indices of the investigated paste mixtures made with different types of admixtures are presented in Fig. 6. As can be observed in Fig. 6a, all the PCE paste mixtures showed a rheopectic behavior (negative A_{thix} values), excluding P22 proportioned with the lowest W/P of 0.30. This suggests that low W/P can lead to thixotropic behavior in presence of PCE admixture, which is in agreement with literature [50]. Indeed, high W/P can lead to a reduction in shear strength properties. Moreover, the PCE-based mixtures containing high specific surface area Clay Type II showed greatly negative A_{thix} values, reflecting a rheopectic behavior. On the other hand, the PNS-based paste mixtures proportioned with Clay Type II and low W/P showed great thixotropic behaviors, as illustrated in Fig. 6b. However, the thixotropic behavior of the mixture P32 turned to rheopexy over time. This can be due to its relatively higher W/P compared to P26 and P44, despite their comparable clay contents. As for the PNS-based paste mixtures containing Clay Type I, the mixtures P10 and P23 showed the lowest rheopexy values due to their low W/P. Regardless to the clay type, the mixtures P10 and P26 proportioned with the lowest W/P of 0.30 exhibited the highest A_{thix} rates over time.

As can be observed in Fig. 6c, all the NE-PC-based paste mixtures showed thixotropic behavior (positive A_{thix} values), regardless of the clay type. Among the NE-PC mixtures, the highest A_{thix} value was obtained for the mixture P45, which is the only mixture proportioned with fine Clay Type II. This suggests the higher contribution of the powder constituents on the A_{thix} of NE-PC-based mixtures compared to their W/P. However, the contribution of these influencing parameters on A_{thix} and its variation over time remained questionable and need to be further investigated. The only system dispersed with NaHMP (P25) showed a higher rheopectic behavior comparable to that of the PCE-based paste mixtures proportioned with Clay Type II. The high rheopectic behavior observed for the mixture P25 can be attributed to the synergy between NaHMP and Clay Type I.

The workability and rheological results of the investigated paste mixtures are summarized in Table 4. The flow curves were evaluated using both Bingham and Herschel-Bulkley models. As can be observed, all the investigated earth-based paste mixtures exhibited a shear-thinning behavior, reflected by pseudoplastic indices "n" lower than 1, excluding the mixture P23 proportioned with the highest content of Clay Type I ($n_{P23} = 1.06$). However, it must be noted that the use of Bingham model led to coefficient of determinations R^2 higher than 0.94, excluding the mixtures P17, P25, P37, and P49 which showed the highest rheopectic behavior. Moreover, relatively high consistency indices "k" were obtained for these mixtures. The Bingham model was applied to assess the evolution of viscoplastic properties (yield stress and plastic viscosity) of all the investigated mixtures because of its conformity with the majority of mixtures. Furthermore, significantly high yield stress and plastic viscosity values were obtained for the mixture P25 made with NaHMP. This can be attributed to the synergy between NaHMP and the ternary binder system (cement, clay, and silt). The clay type showed the second degree of significance on rheological parameters. Accordingly, high viscoplastic properties were obtained for the mixtures proportioned with Clay Type II.

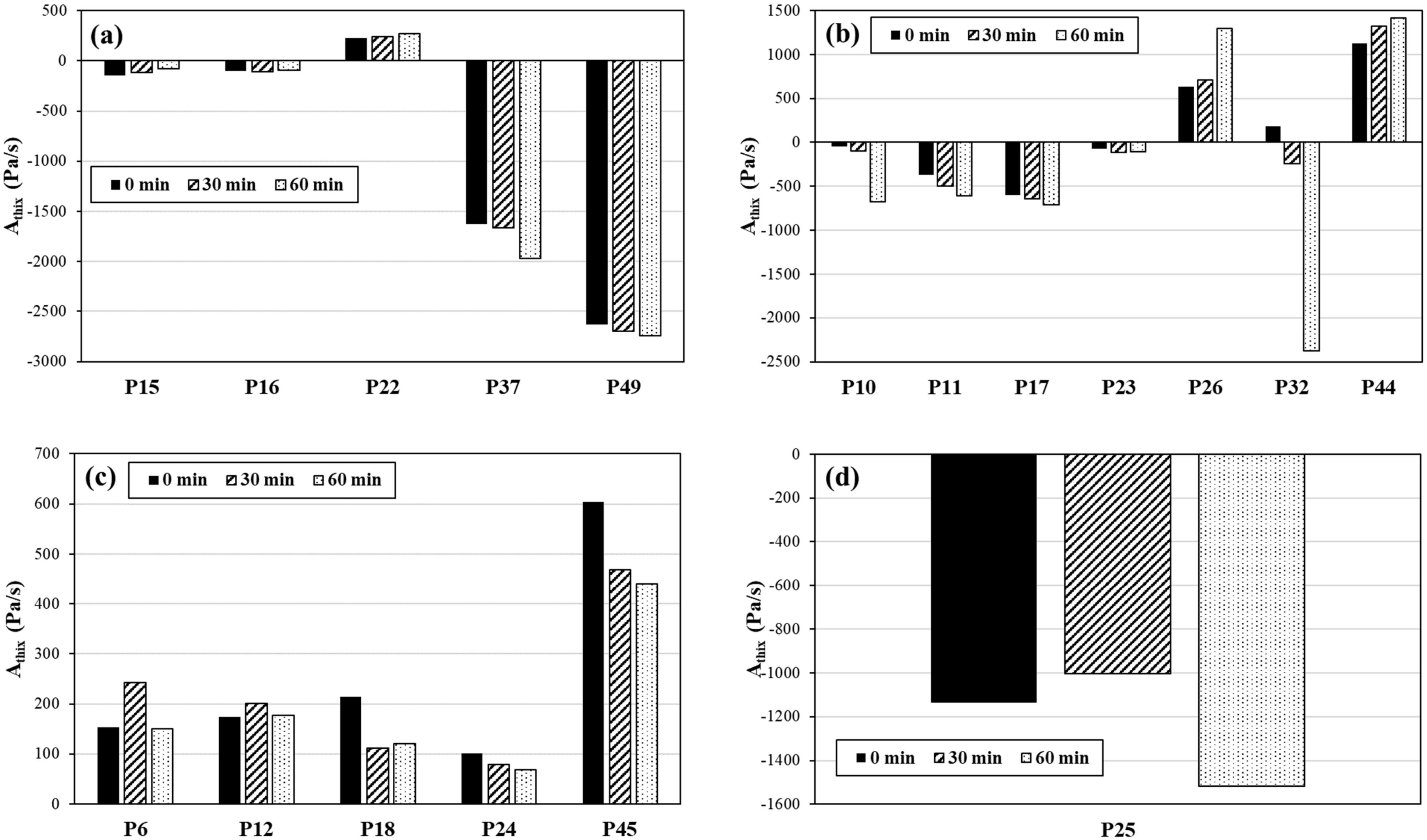

Fig. 6. A_{thix} values of the investigated paste mixtures proportioned with (a) PCE, (b) PNS, (c) NE-PC, and (d) NaHMP admixtures.

267

Table 4. Workability and rheological properties of the investigated paste mixtures.

Mix No.	Clay type	Admixture type	MSF (mm)			MCT (s)	Bingham model							Herschel-Bulkley model										
							0 min			30 min		60 min		0 min				30 min			60 min		
			0 min	30 min	60 min	0 min	τ_0 (Pa)	μ_p (Pa.s)	R^2	τ_0 (Pa)	μ_p (Pa.s)	τ_0 (Pa)	μ_p (Pa.s)	τ_0 (Pa)	k (Pa.s^n)	n	R^2	τ_0 (Pa)	k (Pa.s^n)	n	τ_0 (Pa)	k (Pa.s^n)	n
P6		NE-PC	286	272	267	27	3.8	0.42	0.998	3.3	0.42	4.0	0.42	2.2	0.68	0.91	1.000	1.9	0.63	0.92	2.2	0.69	0.90
P10		PNS	292	209	189	29.0	9.9	0.87	0.966	18.9	0.97	31.9	1.19	4.2	1.83	0.85	1.000	8.4	3.02	0.78	13.2	5.47	0.71
P11		PNS	281	234	205	11.0	18.2	0.29	0.944	22.8	0.32	29.5	0.38	8.4	3.64	0.52	0.996	8.8	5.90	0.45	1.0	15.51	0.32
P12		NE-PC	293	277	261	25.0	14.0	0.17	0.984	15.6	0.18	19.5	0.19	11.6	0.70	0.73	0.998	13.1	0.73	0.73	15.8	1.11	0.66
P15		PCE	279	260	248	17.0	10.8	0.43	0.990	14.1	0.46	18.0	0.53	6.1	1.37	0.78	0.999	7.6	1.86	0.73	8.5	2.82	0.68
P16	Type I	PCE	280	231	213	21.0	17.0	0.18	0.970	19.5	0.20	22.4	0.22	13.1	1.21	0.63	0.999	14.8	1.52	0.61	16.9	1.84	0.59
P17		PNS	283	221	209	11.0	43.8	0.29	0.634	48.2	0.37	61.6	0.46	0.0	29.08	0.21	0.952	0.0	30.29	0.24	0.0	39.16	0.23
P18		NE-PC	286	270	252	26.0	6.5	0.80	0.998	6.6	0.80	8.6	0.87	2.7	1.38	0.89	1.000	2.9	1.38	0.89	3.6	1.68	0.87
P22		PCE	283	256	238	36.0	10.0	0.65	0.968	11.0	0.71	13.1	0.75	2.9	2.04	0.78	0.979	7.5	1.27	0.89	8.6	1.49	0.87
P23		PNS	295	195	148	41.0	3.9	0.53	0.999	8.0	0.58	10.1	0.67	5.1	0.40	1.06	1.000	4.8	1.11	0.87	10.8	0.58	1.03
P24		NE-PC	286	267	238	28.0	11.6	0.23	0.993	13.2	0.24	16.5	0.26	9.7	0.56	0.83	0.999	10.9	0.67	0.80	13.7	0.83	0.78
P25		NaHMP	294	100	100	81.0	114.6	0.97	0.640	123.9	1.32	127.9	1.43	0.0	70.28	0.25	0.948	0.0	71.85	0.29	0.0	73.06	0.29
P26		PNS	276	249	219	16.0	7.4	1.18	0.998	10.6	1.28	21.9	1.50	1.7	2.08	0.89	1.000	3.7	2.39	0.88	8.4	3.97	0.81
P32		PNS	282	250	216	45.0	33.4	0.67	0.979	65.0	0.80	133.1	1.06	22.0	3.37	0.69	0.999	31.4	13.78	0.47	0.0	88.57	0.22
P37	Type II	PCE	286	259	237	56.0	60.3	0.59	0.838	74.7	0.73	94.6	0.88	0.0	36.88	0.26	0.998	0.0	45.72	0.26	0.0	58.89	0.25
P44		PNS	269	239	219	61.0	26.1	1.40	0.996	34.8	1.47	51.6	1.57	17.7	2.79	0.87	1.000	24.6	3.22	0.85	37.0	4.29	0.81
P45		NE-PC	284	269	250	34.0	16.2	0.58	0.992	13.2	0.58	13.3	0.61	10.7	1.61	0.80	0.999	8.3	1.46	0.82	8.4	1.49	0.83
P49		PCE	272	163	138	51.0	76.3	0.84	0.851	113.5	1.21	131.1	1.37	0.0	44.60	0.29	0.999	0.0	67.17	0.28	0.0	78.23	0.28

Flow curves of the investigated paste mixtures with the non-linear shear-thinning behavior are presented in Fig. 7. Despite the comparable mixture constituents, the mixtures P25 (NaHMP admixture) and P17 (PNS admixture) exhibited the highest and lowest rheological parameters, respectively. The presence of PNS in the mixture P17 proportioned with the highest water content led to non-linear viscoplastic behavior. It is worth mentioning that the mixture P17 was made with Clay Type I having low PI value of 3.8%. This suggests that the observed non-linearity is not due to the type and content of clay used. However, the clay type and content significantly affected the rheological behavior of the PCE mixtures. Accordingly, the mixtures P37 and P49, exhibiting the highest PI values (11% for both) among the PCE-based mixtures, showed significant nonlinear viscoplastic behavior, even more than the mixture P17. High PI values can reflect the high specific surface area of the incorporated earth, which induces higher water absorption, nucleation promotion, and flocculation [22]. It must also be noted that the effect of very fine particles on stiffening can be attenuated due to the breakage of the flocs [51]. Therefore, the admixture type and its sensitivity to clay or water content dictate the rheological behavior of the self-consolidating paste mixtures.

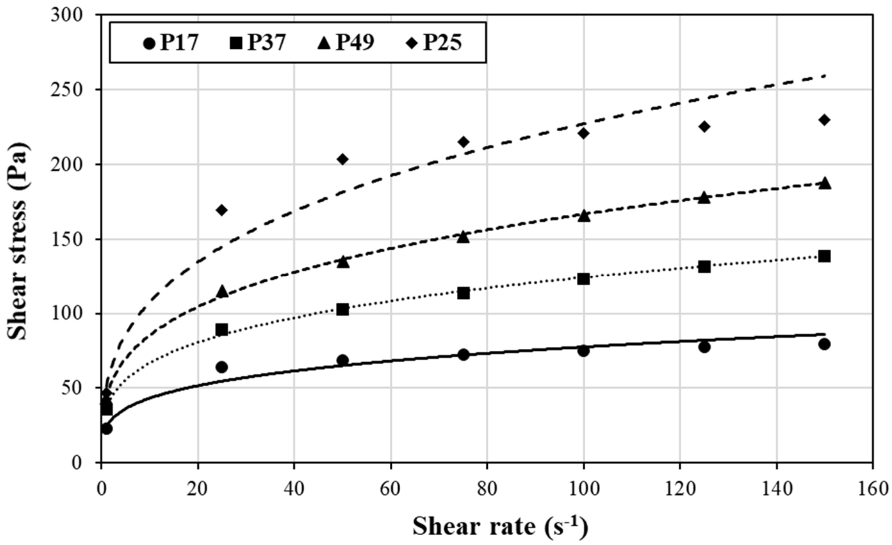

Fig. 7. Flow curves of the paste mixtures P17, P37, P49, and P25.

It is worth mentioning that all the rheological measurements were carried out on the paste mixtures having a MSF of 280 ± 20 mm. Although the use of Herschel-Bulkley model resulted in better fitting, the Bingham parameters were discussed here for comparison purposes. The Bingham yield stress and plastic viscosity of the PCE paste mixtures are presented in Fig. 8. As can be observed, the mixtures P37 and P49 made with Clay Type II (i.e., higher specific surface area and PI) showed the highest yield stress values due to the significant effect of Clay Type II. The PI values of the incorporated earth types showed a significant effect on yield stress values of the PCE-based mixtures. For example, the PCE mixture made with Clay Type I and low PI values (less than 4%) exhibited comparable yield stress values. All these mixtures exhibited yield stress values less than 20 Pa with low increasing rate. However, the highest yield stress value among the PCE-Clay Type I-based mixtures was obtained for the mixture P16 with relatively higher PI value than that of the P15 and P22 mixtures. On the other hand, the plastic viscosity values were found highly affected by W/P. As can be observed in Fig. 8, among the PCE mixtures proportioned with Clay Types I and II, the P16 and P22 (Clay Type I), and P37 and P49 (Clay Type II) showed the lowest and highest plastic viscosity values, respectively, which is probably due to the W/P. Hence, it can be concluded that the yield stress and plastic viscosity of the mixtures containing PCE mostly governed by clay type/content (PI values) and W/P, respectively.

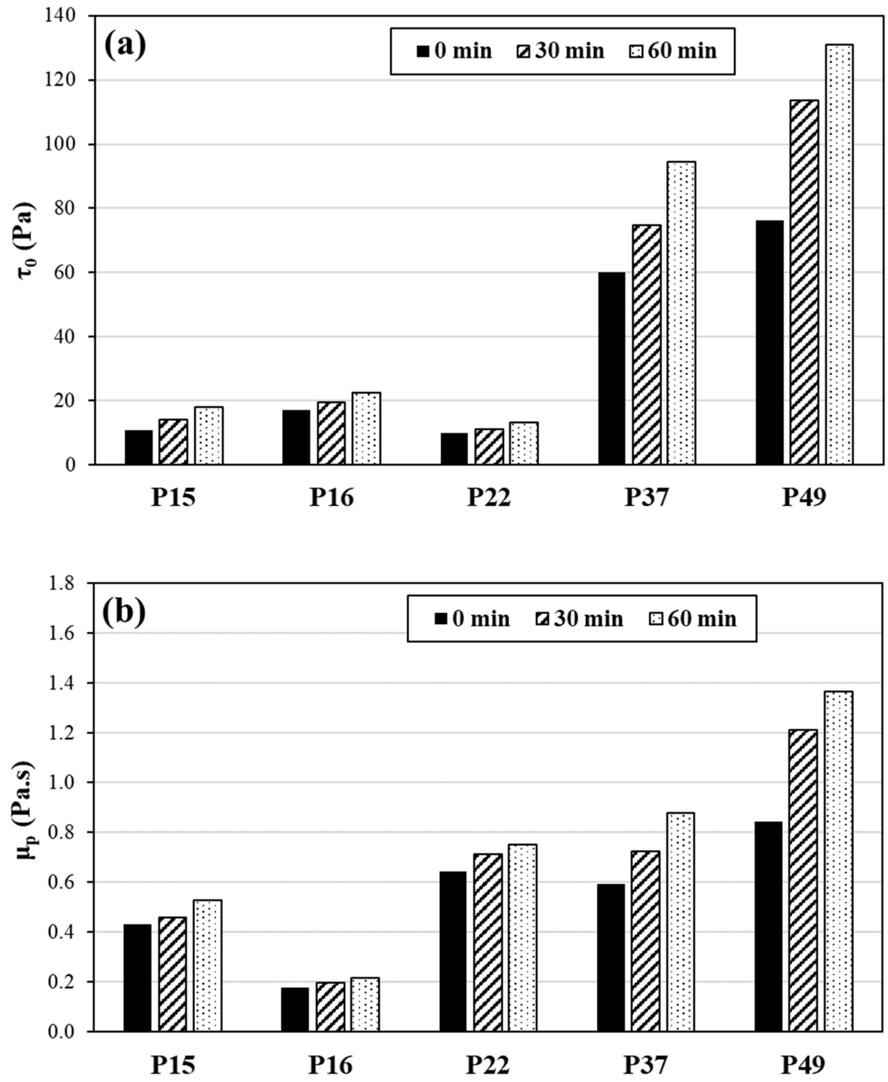

Fig. 8. Bingham rheological parameters of the PCE paste mixtures, including (a) yield stress and (b) plastic viscosity.

As shown in Fig. 9, the yield stress of the paste mixtures proportioned with PNS admixture were found to be dependent on the coupled effect of clay type/content and W/P. As can be observed, despite its higher W/P, the mixture P32 exhibited the highest yield stress values and increasing rate over time rather than the mixtures P44 and P26. This can confirm the coupled contribution of clay and water on yield stress of the mixtures containing PNS. It must be noted that applying the Bingham model for the P17 mixture (Fig. 9) resulted in untrustworthy results compared to other mixtures (low R^2 value of 0.63). Therefore, among the paste mixtures proportioned with PNS and Clay Type I, excluding P17, the mixture P11 showed the highest yield stress value despite its relatively higher W/P of 0.40 compared to the P10 and P23 mixtures. However, unlike the yield stress values, lower plastic viscosity values were obtained for the paste mixtures proportioned with higher W/P. Accordingly, among the Clay Type I-based paste mixtures, the mixture P10 exhibited the highest plastic viscosity due to its lowest W/P of 0.3. Similarly for the Clay Type II-based mixtures, the lowest plastic viscosity value was obtained for the mixture P32 made with the highest W/P. Hence, it can be concluded that the yield stress values of the PNS-dispersed paste mixtures were more influenced due to their water content compared to those proportioned with the PCE admixture. However, the plastic viscosity values of the PCE- and PNS-based mixtures showed comparable sensitivities due to W/P variations.

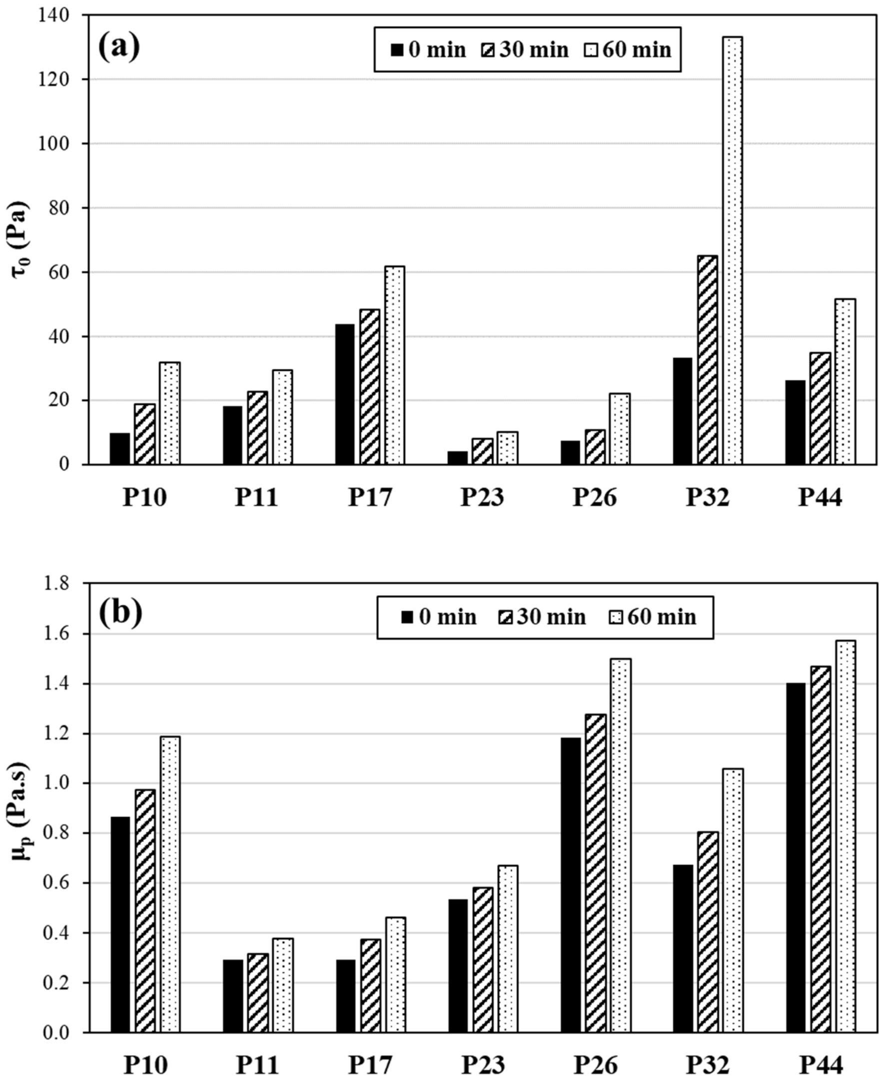

Fig. 9. Bingham rheological parameters of the PNS paste mixtures, including (a) yield stress and (b) plastic viscosity.

As can be observed in Fig. 10, the use of NE-PC led to significantly lower values and increasing rates of yield stress over time (less than 20 Pa after 60 min) rather than those obtained using the PCE and PNS admixtures. Among the NE-PC-contained paste mixtures, the mixture P6 exhibited the lowest yield stress which is due to its lowest clay content. However, similar to other admixtures, the plastic viscosity values of the NE-PC-based paste mixtures were mostly controlled by W/P. Accordingly, the mixture P18 exhibited the highest plastic viscosity value due to its lowest W/P of 0.30. On the other hand, although the mixtures P24 and P45 were proportioned with a fixed W/P of 0.40, the mixture P45 showed higher plastic viscosity than P24. This can be due to its higher PI value (11.8% vs. 7.1%), hence reflecting the effect of clay type on plastic viscosity values. Due to the coupled effect of influencing parameters affecting the rheological parameters, further investigation was required to understand the significance of each factor.

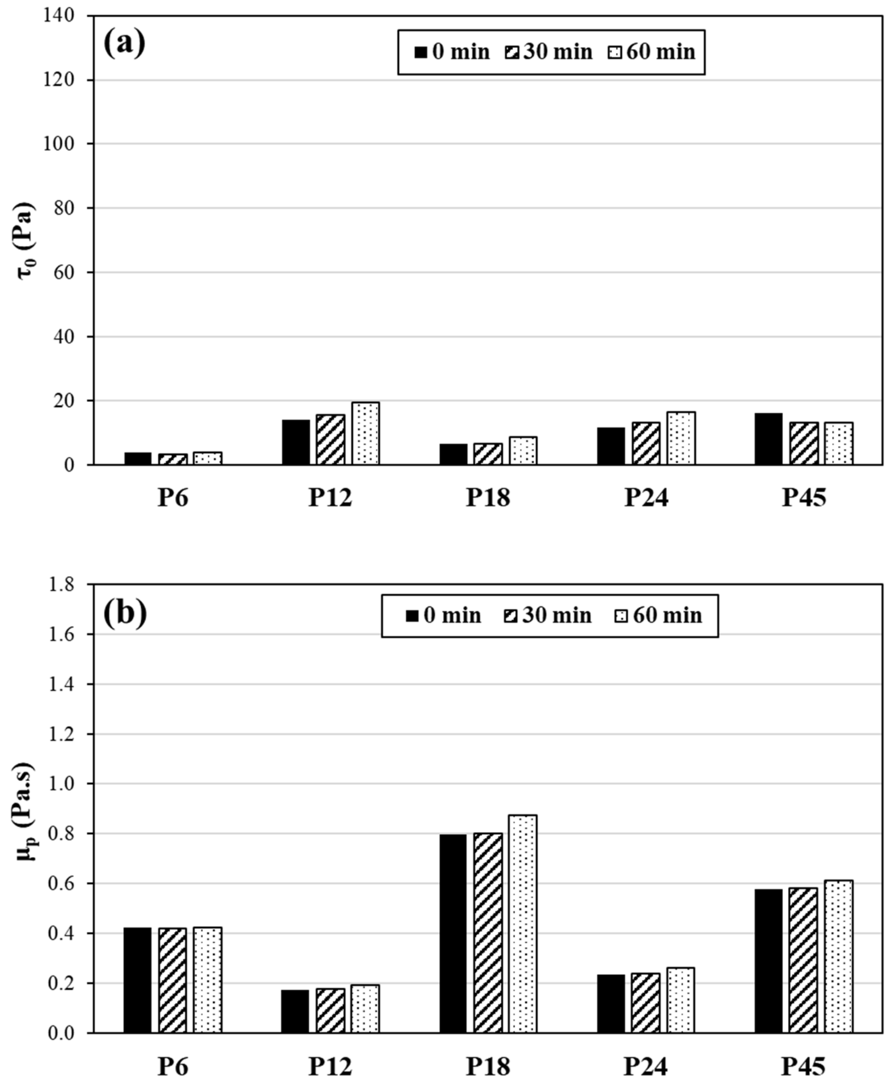

Fig. 10. Bingham rheological parameters of the NE-PC paste mixtures, including (a) yield stress and (b) plastic viscosity.

3.2. Rheology of CEM mixtures

The workability and rheological measurements results of the investigated CEM mixtures are summarized in Table 5. As can be observed, simultaneous incorporation of Clay Type II and PNS admixture led to low flowability reflected by MSF values lower than the targeted value 280 ± 20 mm. This can reflect the incompatibility between the PNS admixture and Clay Type II. Furthermore, the mixture M6, containing high content of silt, showed extensive segregations prior achieving the targeted MSF. It is worth mentioning that rheological behavior of all the mixtures was well-fitted with the Bingham model, excluding the mixture M25. Indeed, the mixture M25, proportioned with NaHMP admixture, showed quite high shape stability, reflected by significantly higher values and increasing rates of yield stress and plastic viscosity over time, rather than other mixtures. Accordingly, no flow was recorded for the mixture M25 through the MVF (blockage) and MSF (no spread) tests. Such shape stability is highly favorable for concrete 3D-printing applications.

Table 5. Workability and rheological properties of the investigated CEM mixtures over time.

Mix No.	Clay type	Admixture type	MSF (mm)			MVF (s)			Bingham parameters					
									0 min		30 min		60 min	
			0 min	30 min	60 min	0 min	15 min	30 min	τ_0 (Pa)	μ_p (Pa.s)	τ_0 (Pa)	μ_p (Pa.s)	τ_0 (Pa)	μ_p (Pa.s)
M6	Type I	NE-PC	NA	-	-	-	-	-	-	-	-	-	-	-
M10		PNS	265	222	155	7.1	11.5	18.2	15.3	5.26	42.6	11.51	75.7	22.43
M11		PNS	269	236	193	3.2	3.9	4.4	35.8	3.69	52.6	4.77	66.6	6.18
M12		NE-PC	266	259	238	1.5	1.9	2.4	17.0	1.11	22.0	1.86	26.2	3.31
M15		PCE	279	243	211	2.4	3.1	3.7	21.8	1.42	29.8	2.80	36.9	3.96
M16		PCE	272	236	189	3.0	3.6	4.1	22.1	2.85	31.8	3.67	48.8	4.80
M17		PNS	263	223	156	1.0	1.7	2.1	37.9	1.02	56.2	1.68	71.6	2.99
M18		NE-PC	265	261	248	9.9	11.0	13.5	12.4	7.09	16.5	11.16	23.5	21.12
M22		PCE	282	264	249	7.5	7.9	8.3	31.4	7.41	46.4	9.15	54.9	10.80
M23		PNS	264	232	171	3.3	4.3	10.9	41.6	3.12	68.4	5.02	82.8	12.67
M24		NE-PC	281	267	246	3.1	4.0	5.2	21.4	3.19	27.3	5.02	32.9	6.42
M25		NaHMP	263	100	100	2.0	blocked	blocked	182.1	9.53	744.9	38.24	849.4	42.56
M26	Type II	PNS	NA	-	-	-	-	-	-	-	-	-	-	-
M32		PNS	NA	-	-	-	-	-	-	-	-	-	-	-
M37		PCE	286	209	171	2.5	3.6	4.2	47.7	5.17	81.9	6.01	121.9	8.15
M44		PNS	NA	-	-	-	-	-	-	-	-	-	-	-
M45		NE-PC	264	250	247	2.7	3.7	4.3	53.0	5.57	62.5	6.85	68.3	9.04
M49		PCE	270	201	184	2.2	5.6	8.4	85.2	4.82	102.5	8.83	149.1	15.93
M_{ref}	-	PCE	273	240	195	2.9	5.3	5.8	24.6	3.58	29.5	4.78	38.5	6.12

NA: Not achieved to the targeted MSF of 280 ± 20 mm

The Bingham yield stress and plastic viscosity of the CEM mixtures dispersed with the PCE are presented in Fig. 11. As can be observed, the results of the PCE-based CEM mixtures were comparable to their corresponding paste mixtures in which M49 followed by M37 showed the highest yield stress values (more than 40 Pa at t = 0). As discussed earlier, this is due to their high contents of Clay Type II (high PI values). On the other hand, the mixtures containing the Clay Type I exhibited almost comparable yield stress values (less than 40 Pa at t = 0). This can be due to the coupled effect of clay type/content, W/P, and EP thickness on yield stress of the PCE-based mortar mixtures. The contributions of these influencing parameters are discussed further in Section 3.4. However, immediately after mixing, among all the PCE-based CEM mixtures, the mixture M22 showed the highest plastic viscosity value which can be due to its lowest W/P of 0.30. It can confirm higher contribution of W/P on plastic viscosity of the PCE-based mixtures, rather than binder composition. Moreover, higher increasing rates of plastic viscosity values obtained for the mixture P49 can be explained due to its lower W/P and e_{EP}, compared to the mixture P37.

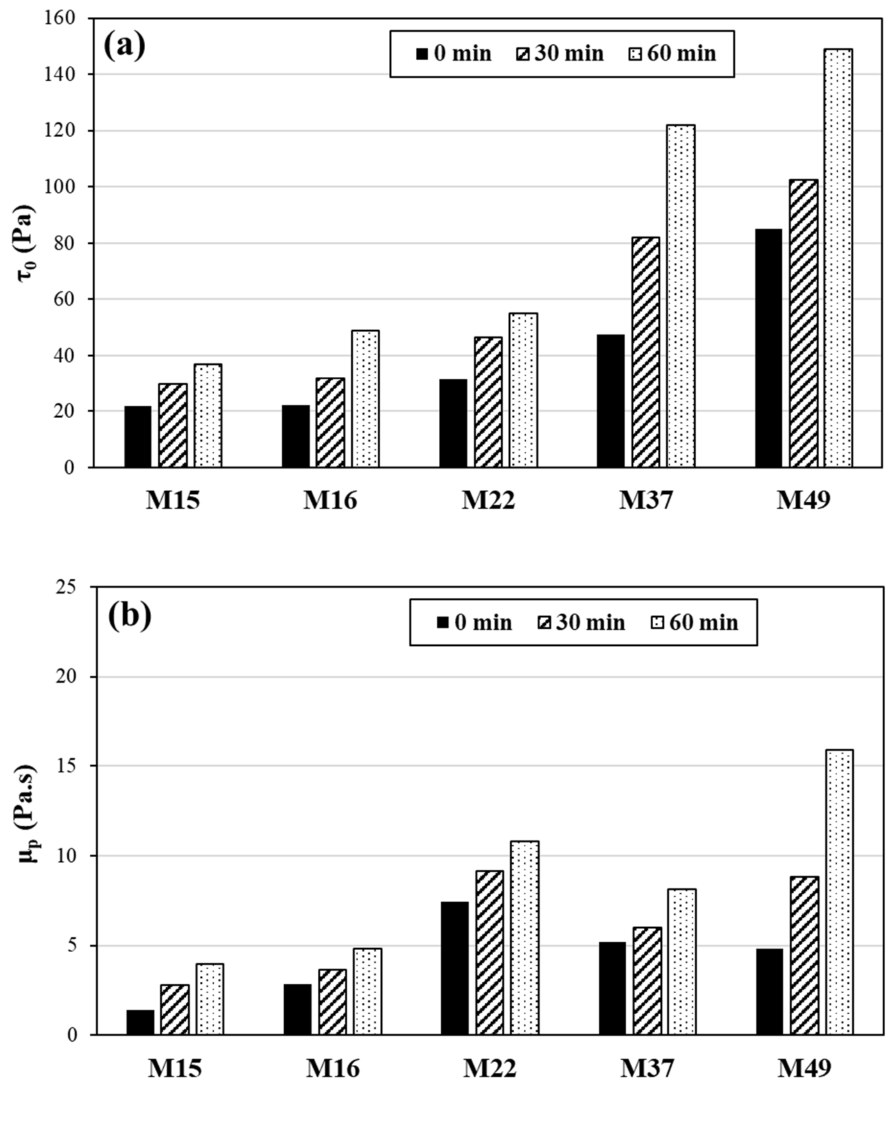

Fig. 11. Bingham (a) yield stress and (b) plastic viscosity of the PCE-contained CEM mixtures.

The Bingham yield stress and plastic viscosity of the PNS-contained CEM mixtures over time are illustrated in Fig. 12. As mentioned earlier, the PNS-Clay Type II CEM mixtures could not achieve the targeted MSF of 280 ± 20 mm. Therefore, only the results of the PNS-Clay Type I-based CEM mixtures were discussed in this section. As can be observed, all these mixtures showed an initial yield stress values lower than 40 Pa at t = 0. The plastic viscosity of the PNS-based CEM mixtures was mainly controlled by the W/P, while the yield stress was affected by the clay type/content, W/P, and EP thickness. Further discussions will be provided in Section 3.4. Among all the PNS-Clay Type I-based CEM mixtures, the mixtures M10 and M17 showed the highest and lowest plastic viscosity values due to their lowest and highest W/P of 0.30 and 0.50, respectively. Moreover, similarly to the PCE-dispersed CEM mixtures, the highest increasing rate of plastic viscosity values was obtained for the mixtures M10 and M23 proportioned with the lowest W/P of 0.30 and 0.35, respectively.

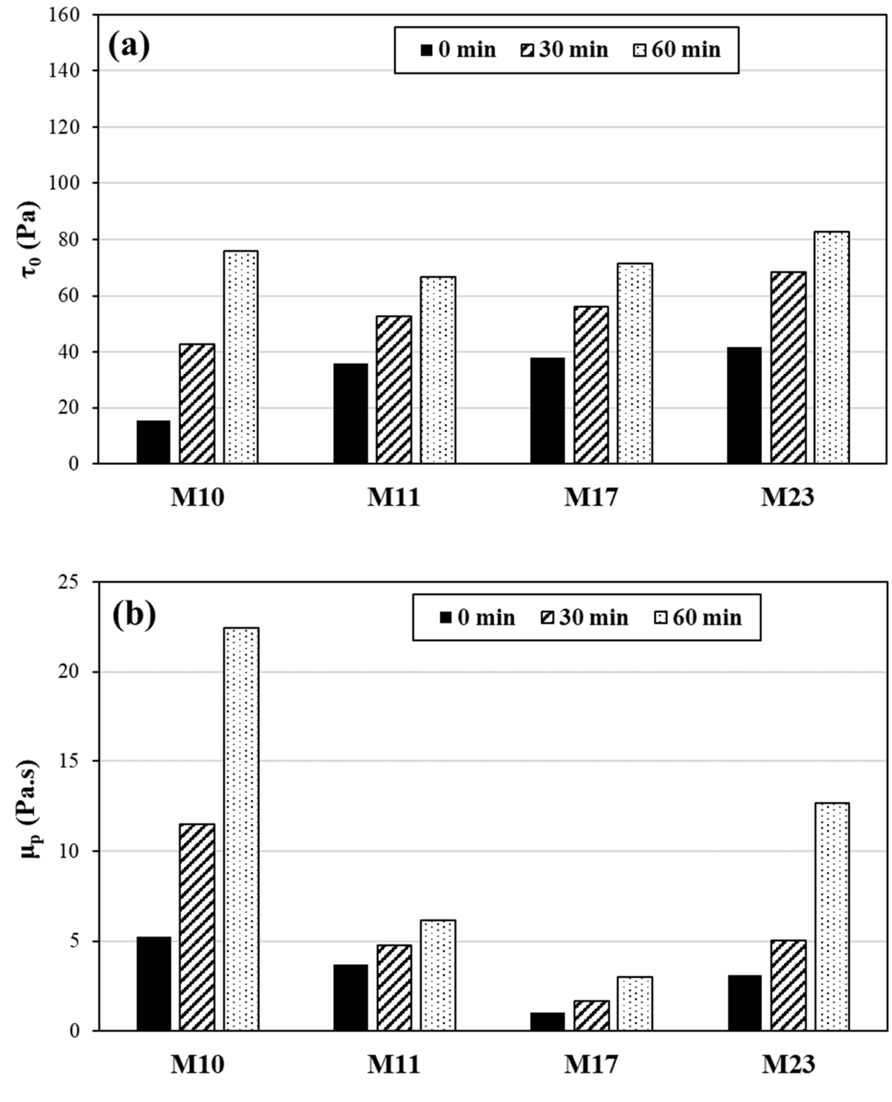

Fig. 12. Bingham (a) yield stress and (b) plastic viscosity of the PNS-contained CEM mixtures.

As can be observed in Fig. 13, the mixture M45 exhibited the highest yield stress value among all the NE-PC-based CEM mixtures due to its finer Clay Type II. This can be generally concluded that regardless of the admixture type, all the CEM mixtures proportioned with the Clay Types I and II showed initial yield stress values lower and higher than 40 Pa at t = 0, respectively. Moreover, the values and increasing rates of the yield stress over time of the CEM mixtures dispersed with the NE-PC admixture were found relatively lower than those obtained by incorporating the PNS and PCE admixtures. This can be referred to the synergy of this linear type of PC with powder constituents of the earth binders. The coupled effect of the mixture constituents on the yield stress values of the NE-PC-based CEM mixtures are further discussed in Section 3.4. Moreover, similarly to other types of admixtures, the plastic viscosity of the NE-PC-based CEM mixtures was found to be highly dependent on W/P. Accordingly, the mixtures M12 and M18 showed the lowest and highest plastic viscosity values due to their highest (0.45) and lowest (0.30) W/P, respectively.

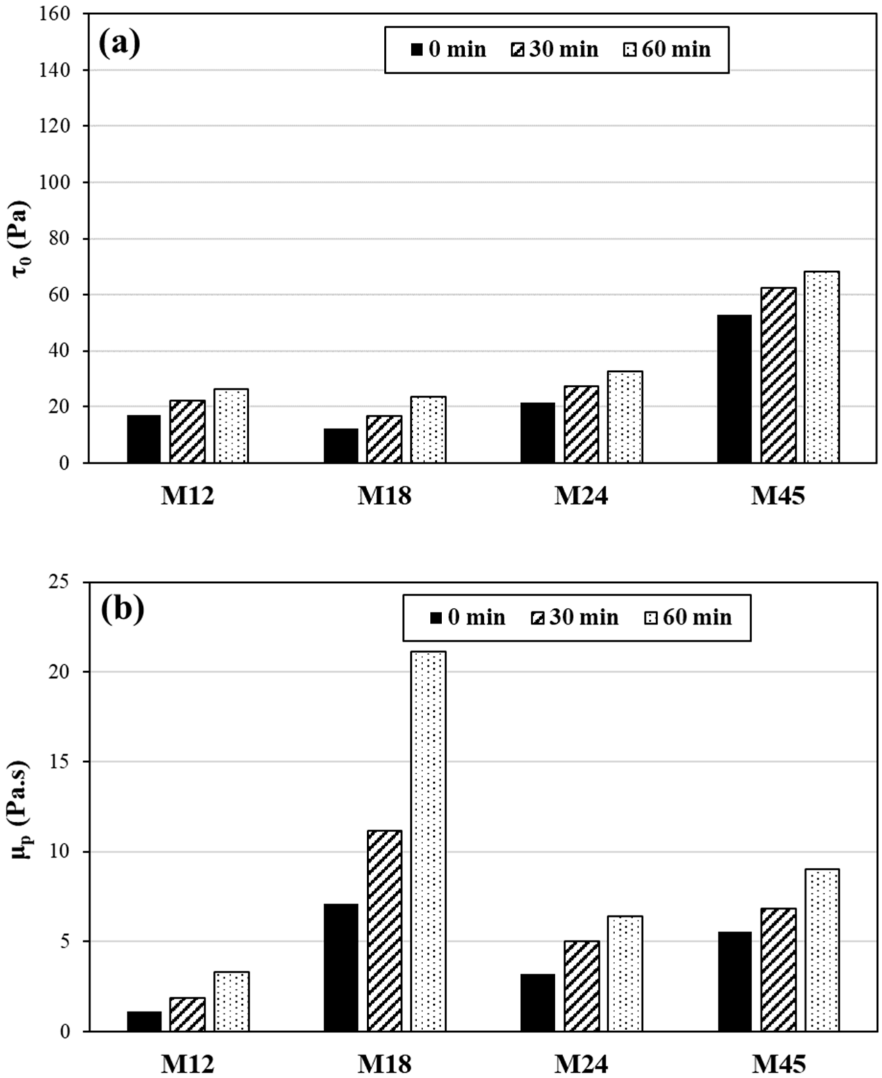

Fig. 13. Bingham (a) yield stress and (b) plastic viscosity of the NE-PC-contained CEM mixtures.

Analysis of variance (ANOVA) was conducted to assess the contribution of the modeled factors on the Bingham yield stress and plastic viscosity of the investigated CEM mixtures determined immediately after mixing (i.e., t = 0). As summarized in Table 6, the yield stress is mainly affected by admixture type, while the significance of W/P and V_P was relatively lower. However, W/P showed the highest contribution on plastic viscosity. In addition to the effect of clay type/content, these contributions are further discussed in Section 3.4.

Table 6. ANOVA analysis for the Bingham yield stress and plastic viscosity of CEM mixtures at t = 0.

Source	Yield stress		Plastic viscosity	
	Contribution (%)	P-Value	Contribution (%)	P-Value
W/P	22.32	0.201	70.13	0.090
V_P	19.60	0.293	7.29	0.283
Admixture type	51.07	0.121	18.70	0.172
Error	7.01		3.88	
Total	100.0		100.0	

3.3. Rheology of SCEC mixtures

The rheometric results revealed that the Bingham model was well fitted to the shear stress-shear rate data of the investigated SCEC mixtures. The workability and rheological properties of the four investigated SCEC mixtures proportioned with PCE are summarized in Table 7. In addition to the Bingham yield stress and plastic viscosity, the workability was assessed in terms of V-Funnel and slump flow measurements.

Table 7. Experimental results of the investigated concrete mixtures.

Mix No.	Admixture type	Workability						Rheological propertied (Bingham model)					
		Slump flow (mm)			V-Funnel (s)			0 min		30 min		60 min	
		0 min	30 min	60 min	0 min	30 min	60 min	τ_0 (Pa)	μ_p (Pa.s)	τ_0 (Pa)	μ_p (Pa.s)	τ_0 (Pa)	μ_p (Pa.s)
C16	PCE	705	665	625	1.6	1.8	1.9	30.7	3.31	37.9	4.71	54.6	5.51
C22	PCE	820	780	732	4.2	4.4	4.7	49.5	9.95	57.0	10.10	64.6	12.18
C37	PCE	805	495	410	2.5	4.0	5.5	49.9	6.10	98.8	7.04	154.3	9.74
C_{ref}	PCE	730	645	610	1.5	3.1	3.2	34.1	5.74	39.9	6.05	51.1	7.09

The Bingham yield stress and plastic viscosity values of the investigate SCEC mixtures are presented in Fig. 14. As can be observed, the mixtures C16 and C_{ref} showed comparable yield stress values, despite their different binder constituents. This can highlight the coupled effect of different influencing parameters, including S/A, W/P, and V_P, as well as content and type of the clay used. Moreover, although the mixtures C22 and C37 exhibited comparable initial yield stress values after mixing (t = 0), the yield stress values of the mixture C37 showed significantly higher increasing rate over time. This is due to its finer clay particles and higher W/P. Furthermore, similarly to the investigated paste and CEM mixtures, W/P was found as the most influencing factor on plastic viscosity values of the investigated PCE-based SCEC mixtures. Accordingly, the mixture C22 with the lowest W/P of 0.30 showed the highest plastic values among all the investigated SCEC mixtures.

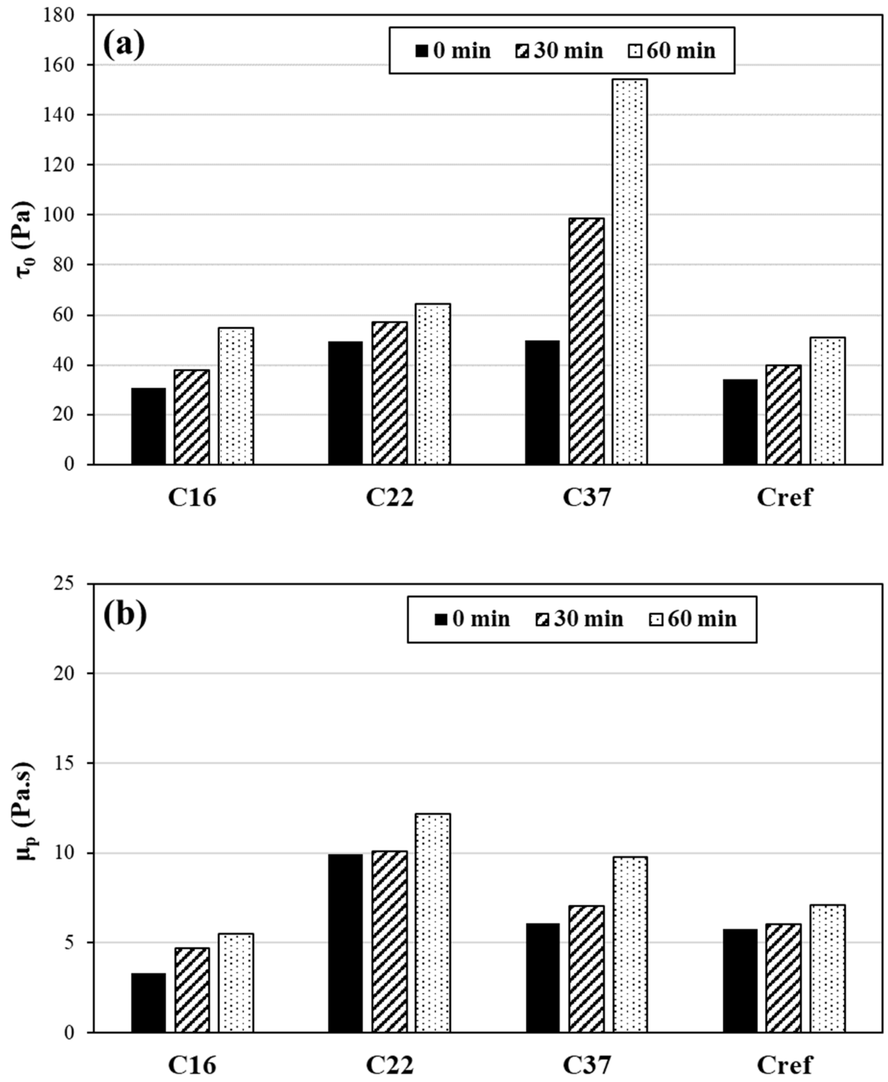

Fig. 14. Bingham (a) yield stress and (b) plastic viscosity of the investigated SCEC mixtures.

3.4. Multiscale approach to control rheology of SCEC

As discussed earlier, the rheology of self-consolidating earth-based cementitious suspensions is tricky due to the presence of clay and silt particles. In order to facilitate the control, prediction, and optimization of the rheological parameters, it is important to investigate the main influencing parameters on rheology of these materials. Also, it is useful to establish relationships between workability and rheology of SCEC and facilitate its design and achieving adequate rheological properties. In this section, the coupled effect of different characteristics of mixture constituents on rheological properties of the investigated SCEC, CEM, and paste mixtures was evaluated. Accordingly, the following correlation was established between different workability and rheological properties (Response) of the investigated mixtures and the main influencing parameters (a_i), indicated in the last section:

$$\text{Response} = \alpha + \beta \times \prod_{i=1}^{n}(a_i^{m_i}) \tag{4}$$

where n is the number of influencing parameters $a_{i\,=\,1\text{ to }n}$, and α, β, and $m_{i\,=\,1\text{ to }n}$ are the adjustment factors which were determined for each "Response" using a developed Microsoft Excel solver. The five influencing parameters $a_{i\,=\,1\text{ to }5}$ included the PI and W/P in the paste mixtures, in addition to V_P and e_{EP} in the CEM mixtures, and S/A in the investigated SCEC mixtures. It is worthy to mention that the effect of the type and content of the clay used on rheological properties of the investigated mixtures was assessed using the PI values of the soil (clay, silt, and sand < 425 µm). The results of the established correlations are summarized in Table 8, in terms of the obtained adjustment factors (α, β, and $m_{i = 1 \text{ to } 5}$). Moreover, the precision of the established predictions was evaluated by considering the estimation index (EI), R^2, and root-mean-square error (RMSE) values, as presented in Table 8. The EI indices were defined as the mean value of the ratio between the predicted and experimental values. It is important to mention that R^2 and EI values closer to unity and lower RMSE values correspond to stronger agreement between the investigated flow performance responses and mixture constituent parameters. The investigated "Responses" included the characteristics of the investigated mixtures in different scales, as follow:

(i) Paste scale: The Bingham yield stress and plastic viscosity values, as well as the ratio of the rheology-to-workability immediately after mixing (t = 0) of the investigated paste mixtures containing different types of admixtures.

(ii) CEM scale: The Bingham yield stress and plastic viscosity of the investigated CEM mixtures immediately after mixing (t = 0), relative to those of their corresponding paste mixtures.

(iii) SCEC scale: The Bingham yield stress and plastic viscosity of the investigated SCEC mixtures immediately after mixing (t = 0), relative to those of their corresponding CEM mixtures.

As can be observed in Table 8, the yield stress of the paste mixtures dispersed with the PCE and PNS admixture types are in good agreements with the PI of their earth and W/P. According to the obtained adjustment factors, the yield stress values of the PCE- and PNS-based paste mixtures were found to be more controlled by PI and W/P, respectively. Moreover, the yield stress values of the NE-PC-based mixtures were found highly dependent on the PI values. This can reveal the significant effect of the type and content of the clay used, whereas W/P showed no contribution on the yield stress values of the NE-PC-based mixtures. However, the W/P showed the most dominant effect on plastic viscosity values of the investigated pastes, regardless of their admixture types.

The prediction of the rheological properties using the workability measurements can lead to easier rheological evaluation rather than using sophisticated commercial rheometers [52]. As can be observed in Table 8, the yield stress values of the investigated paste mixtures can be well predicted using their corresponding MSF values as a function of the PI values, reflecting the characteristics of the binder constituents, and W/P. The yield stress-MSF relationship of the PCE-based paste mixtures was found highly dependent on the powder constituents, reflected by high adjustment factor obtained for PI, whereas W/P showed no contribution. However, W/P showed more significant effect on the yield stress-to-MSF ratios of the pastes proportioned with the PNS and NE-PC admixtures, rather than PI of the used earths. On the other hand, the plastic viscosity values of the investigated paste mixtures, proportioned with different types of admixtures, were found in good agreements with their corresponding MCT values with a significant contribution of W/P, regardless of the PI values of their corresponding earths.

Moreover, the yield stress values of the investigated CEM mixtures relative to those of their corresponding paste mixtures were well correlated to W/P, e_{EP}, and PI values, in a descending order of significance. On the other hand, the relative plastic viscosity values of the CEM mixtures to their corresponding paste mixtures were found highly governed by V_P, followed by W/P and EP thickness, whereas the PI values, as an indication of the binder composition, showed no contribution. The independency of the plastic viscosity of the CEM mixtures to the fineness of the ternary binder system was also observed and discussed in Section 3.2. On the other hand, as shown in Table 8, the rheological properties of the investigated SCEC mixtures can be well predicted using those of their corresponding CEM mixtures proportioned using the proposed approach. The established predictions were found significantly dependent on the e_{EP} and S/A values, in a descending order of significance (R^2 and EI values close to unity and low RMSE). This suggests the high potential of the new proposed CEM approach to simulate the rheological properties of the SCEC mixtures.

Table 8. Adjustment factors and prediction precisions of the established correlations (Eq. 4).

	Response	Adjustment factors							Precision		
		α	β	m_i							
				PI (%)	W/P	V_P (%)	e_{EP} (µm)	S/A	EI	R^2	RMSE
Paste	$\tau_{0\text{-PCE}}$ (Pa)	11.01	0.006	3.053	-2.168	-	-	-	0.995	0.997	2.315
Paste	$\tau_{0\text{-PNS}}$ (Pa)	9.784	1927.6	2.507	10.599	-	-	-	0.949	0.953	5.535
Paste	$\tau_{0\text{-NE-PC}}$ (Pa)	0	3.8593	0.594	0	-	-	-	0.976	0.979	1.769
Paste	$\mu_{p\text{-PCE}}$ (Pa.s)	0.273	4.5E-5	1.683	-5.91	-	-	-	0.978	0.982	0.876
Paste	$\mu_{p\text{-PNS}}$ (Pa.s)	0.342	7.8E-7	1.220	-10.386	-	-	-	0.974	0.979	0.136
Paste	$\mu_{p\text{-NE-PC}}$ (Pa.s)	0	0.009	0.301	-3.403	-	-	-	0.96	0.971	0.100
Paste	$\frac{\tau_{0\text{-PCE}}\ (Pa)}{MSF_{0\text{-PCE}}\ (mm)}$	0.034	0.001	2.298	0	-	-	-	0.98	0.972	0.023
Paste	$\frac{\tau_{0\text{-PNS}}\ (Pa)}{MSF_{0\text{-PNS}}\ (mm)}$	0.035	7.13	2.663	10.965	-	-	-	0.95	0.963	0.020
Paste	$\frac{\tau_{0\text{-NE-PC}}\ (Pa)}{MSF_{0\text{-NE-PC}}\ (mm)}$	0.001	0.064	0.522	1.562	-	-	-	0.997	0.992	0.002
Paste	$\frac{\mu_{p\text{-PCE}}\ (Pa.s)}{MCT_{0\text{-PCE}}\ (s)}$	0	0.004	0	-1.417	-	-	-	0.932	0.951	0.004
Paste	$\frac{\mu_{p\text{-PNS}}\ (Pa.s)}{MCT_{0\text{-PNS}}\ (s)}$	0.018	8.1E-8	0	-10.731	-	-	-	0.852	0.965	0.008
Paste	$\frac{\mu_{p\text{-NE-PC}}\ (Pa.s)}{MCT_{0\text{-NE-PC}}\ (s)}$	0.001	3.8E-4	0	-3.594	-	-	-	0.971	0.969	0.003
CEM	$\frac{\tau_{0\text{-CEM}}\ (Pa)}{\tau_{0\text{-paste}}\ (Pa)}$	1.612	4.888	13.204	-52.576	0	-20.546	-	0.968	0.974	0.59
CEM	$\frac{\mu_{p\text{-CEM}}\ (Pa.s)}{\mu_{p\text{-paste}}\ (Pa.s)}$	6.979	1.5E47	0	-4.331	-27.015	-2.004	-	0.922	0.916	2.015
SCEC	$\frac{\tau_{0\text{-concrete}}\ (Pa)}{\tau_{0\text{-CEM}}\ (Pa)}$	1.218	2.5E-10	0	0	0	6.288	15.159	0.995	0.991	0.161
SCEC	$\frac{\mu_{p\text{-concrete}}\ (Pa.s)}{\mu_{p\text{-CEM}}\ (Pa.s)}$	1.228	14.256	0	0	0	-7.170	-37.952	0.997	0.993	0.071

4. Conclusions

In this study, the rheological properties of the SCEC mixtures were investigated in three different scales of paste, CEM, and concrete. The coupled effect of different mixture constituents, including binder composition (type and content of clay, silt, and cement content), V_P, W/P, S/A, EP thickness, and admixture type on rheological properties of the investigated paste, CEM, and SCEC mixtures were evaluated. It should be noted that the plasticity index (PI) was used as the representative characteristic of soil types used which is affected by the fine particles (especially the type and content of clay). The evolution of rheological properties of the investigated SCEC mixtures containing different soil types was compared with those of a reference SCC mixture. Considering the effect of EP thickness, a new CEM approach was proposed to predict the characteristics of the SCEC mixtures in fresh state. The rheological measurements carried out on the investigated mixtures included the viscoplastic properties (yield stress and plastic viscosity) and thixotropy. According to the experimental results, the following concluding remarks can be pointed out:

- The admixture type showed the major effect on the thixotropic or rheopectic behavior of the investigated self-consolidating earth paste mixtures. All the investigated paste mixtures showed rheopectic behavior except those proportioned with PNS admixture and Clay Type II, as well as the one dispersed using the NE-PC admixture.

- The highest thixotropy response was obtained for the paste mixture proportioned with the highest content of the finer Clay Type II. On the other hand, the highest rheopectic behavior was observed for the mixtures P49 and P37 proportioned with PCE admixture and Clay Type II, as well as the mixture P25 dispersed using the NaHMP.

- The admixture and clay types showed the most significant effect on viscoplastic properties of the investigated mixtures. The mixtures proportioned with NaHMP and Clay Type II exhibited the highest yield stress and plastic viscosity values. Moreover, the paste and CEM mixtures containing the NE-PC admixture exhibited relatively lower values and increasing rates of yield stress over time, compared to those proportioned with the PNS and PCE admixtures.

- The yield stress of the investigated paste, CEM, and SCEC mixtures was influenced by the coupled effect of the content and type of clay and W/P. All the CEM mixtures proportioned with the Clay Types I and II exhibited initial yield stress values lower and higher than 40 Pa, respectively, except the one made with NaHMP. In concrete scale, the use of the Clay Type II led to higher values and increasing rates of yield stress over time. However, the plastic viscosity values were mostly governed by W/P following an inverse-proportional relationship.

- A multiscale approach was proposed to control the rheological properties of SCEC mixtures from their corresponding paste and CEM matrices. The rheological properties of SCEC mixtures were successfully predicted using those of their corresponding CEM mixtures, EP thickness, and S/A. The relative rheological properties of the investigated CEM mixtures to their corresponding paste mixtures were found in good agreements with the V_P and EP thickness values.

5. Declaration of competing interest

The authors declare that they have no known competing financial interests or personal relationships that could have appeared to influence the work reported in this paper.

6. Acknowledgement

The authors wish to thank the financial support of the National Science and Engineering Research Council of Canada (NSERC) and the eight industrial partners participating in the NSERC Chair on Development of Flowable Concrete with Adapted Rheology and their Application in Concrete Infrastructures, held by Professor Ammar Yahia at the Université de Sherbrooke.

Appendix

Particle-size distribution and surface area-to-volume ratio (A_{3D}/V) of sand and gravel are summarized in Table 1A. As can be observed, the A_{3D}/V ratios of sand and gravel were calculated by the summation of the corresponding ratios of each of their corresponding subclasses.

Table 1A. Particle-size distribution and surface area-to-volume ratio (A_{3D}/V) of sand and gravel.

Sieve size range (mm)	Sand			Gravel		
	Volumetric fraction (%)	Surface area-to-volume ratio (A_{3D}/V) (m^2/m^3)	A_{3D}/V for each subclass (m^2/m^3)	Volumetric fraction (%)	Surface area-to-volume ratio (A_{3D}/V) (m^2/m^3)	A_{3D}/V for each subclass (m^2/m^3)
10-14	-	-	-	18.3	637	116.6
5-10	4.45	1 125	50.1	71.2	735	523.3
2.5-5	10.41	1 403	146.1	5.4	1 404	75.8
1.25-2.5	14.32	2 963	424.3	5.1	2 825	144.1
0.630-1.25	19.03	11 813	2248.0	-	-	-
0.315-0.630	27.45	19 967	5480.9	-	-	-
0.160-0.315	18.44	50 729	8783.1	-	-	-
0.080-0.160	5.78	74 026	4278.7	-	-	-
0-0.080	0.12	143 499	172.2	-	-	-
TOTAL	100		21583.4	100		859.8

7. References

[1] F. Pacheco-Torgal, S. Jalali, Earth construction: Lessons from the past for future eco-efficient construction, Constr. Build. Mater. 29 (2012) 512–519. https://doi.org/10.1016/j.conbuildmat.2011.10.054.

[2] P. Walker, V. Maniatidis, A Review of Rammed Earth Construction, United Kingdom, 2003.

[3] M. Kohandelnia, M. Hosseinpoor, A. Yahia, R. Belarbi, Hygrothermal and microstructural characterization of self-consolidating earth concrete (SCEC), J. Build. Eng. 69 (2023) 106287. https://doi.org/10.1016/J.JOBE.2023.106287.

[4] R. Bahar, M. Benazzoung, S. Kenai, Performance of compacted cement stabilized soil, Cem. Concr. Compos. 26 (2004) 811–820.

[5] L. Miccoli, U. Müller, P. Fontana, Mechanical behaviour of earthen materials: A comparison between earth block masonry, rammed earth and cob, Constr. Build. Mater. 61 (2014) 327–339. https://doi.org/10.1016/j.conbuildmat.2014.03.009.

[6] M. Kohandelnia, M. Hosseinpoor, A. Yahia, R. Belarbi, A new approach for proportioning self-consolidating earth paste (SCEP) using the Taguchi method, Constr. Build. Mater. 347 (2022) 128579. https://doi.org/10.1016/J.CONBUILDMAT.2022.128579.

[7] M. Kohandelnia, M. Hosseinpoor, A. Yahia, R. Belarbi, Multiscale investigation of self-consolidating earthen materials using a novel concrete-equivalent mortar approach, Constr. Build. Mater. 370 (2023) 130700. https://doi.org/10.1016/J.CONBUILDMAT.2023.130700.

[8] D. Gélard, Identification and Characterization of Internal Cohesion of Earth Material in its Natural Condition (in French), in: INPG Grenoble, France, 2005.

[9] C.M. Ouellet-Plamondon, G. Habert, Self-Compacted Clay based Concrete (SCCC): Proof-of-concept, J. Clean. Prod. 117 (2016) 160–168. https://doi.org/10.1016/j.jclepro.2015.12.048.

[10] A.W. Skempton, The Colloidal activity of clays, in: 3rd Int. Conf. Soil Mech. Found. Eng., London, 1953: pp. 47–61.

[11] B. Voight, Correlation between Atterberg plasticity limits and residual shear strength of natural soils, Géotechnique. 23 (1973) 265–267.

[12] A. Laskar, S.K. Pal, Geotechnical characteristics of two different soils and their mixture and relationships between parameters, Electron. J. Geotech. Eng. 17 (2012) 2821–2832.

[13] P.P. Raj, Soil Mechanics and Foundation Engineering, Dorling Kindersley, (India) Pvt. Ltd., New Delhi, 2012.

[14] M. Westerholm, B. Lagerbald, J. Silfwerbrand, E. Forssberg, Influence of fine aggregate characteristics on the rheological properties of mortars, Cem. Concr. Compos. 30 (2008) 274–282.
[15] S.K. Ling, A.K.H. Kwan, Adding ground sand to decrease paste volume, increase cohesiveness and improve passing ability of SCC, Constr. Build. Mater. 84 (2015) 46–53.
[16] J.J. Chen, B.H. Li, P.L. Ng, A.K.H. Kwan, Adding granite polishing waste as sand replacement to improve packing density, rheology, strength and impermeability of mortar, Powder Technol. 364 (2020) 404–415.
[17] F. Andreola, E. Castellini, J.M.F. Ferreira, S. Olhero, M. Romagnoli, Effect of sodium hexametaphosphate and ageing on the rheological behaviour of kaolin dispersions, Appl. Clay Sci. 31 (2006) 56–64. https://doi.org/10.1016/j.clay.2005.08.004.
[18] F. Andreola, E. Castellini, T. Manfredini, M. Romagnoli, The role of sodium hexametaphosphate in the dissolution process of kaolinite and kaolin, J. Eur. Ceram. Soc. 24 (2004) 2113–2124. https://doi.org/10.1016/S0955-2219(03)00366-2.
[19] F. Andreola, E. Castellini, G. Lusvardi, L. Menabue, M. Romagnoli, Release of ions from kaolinite dispersed in deflocculant solutions, Appl. Clay Sci. 36 (2007) 271–278. https://doi.org/10.1016/j.clay.2006.10.002.
[20] A. Perrot, D. Rangeard, A. Pierre, Structural built-up of cement-based materials used for 3D-printing extrusion techniques, Mater. Struct. 49 (2016) 1213–1220.
[21] A. Mostafa, A. Yahia, New approach to assess build-up of cement-based suspensions, Cem. Concr. Res. (2016) 174–182. https://doi.org/https://doi.org/10.1016/j. cemconres.2016.03.005.
[22] Y. Qian, G. De Schutter, Enhancing thixotropy of fresh cement pastes with nanoclay in presence of polycarboxylate ether superplasticizer (PCE), Cem. Concr. Res. 111 (2018) 15–22. https://doi.org/10.1016/J.CEMCONRES.2018.06.013.
[23] Q. Yuan, X. Lu, K.H. Khayat, D. Feys, C. Shi, Small amplitude oscillatory shear technique to evaluate structural build-up of cement paste, Mater. Struct. 50 (2016) 112. https://doi.org/10.1617/s11527-016-0978-2.
[24] R. Ferron, A. Gregori, Z. Sun, S.P. Shah, Rheological method to evaluate structural buildup in self-consolidating concrete cement pastes, ACI Mater. J. 104 (2007) 242–250.
[25] Y. Zhang, Y. Zhang, W. She, L. Yang, G. Liu, Y. Yang, Rheological and harden properties of the high-thixotropy 3D printing concrete, Constr. Build. Mater. 201 (2019) 278–285. https://doi.org/10.1016/J.CONBUILDMAT.2018.12.061.
[26] A. Kaleta-Jurowska, S. Grzeszczyk, M. Dziubiński, Application of multiple step change in shear rate model for determination of thixotropic behaviour of cement pastes, J. Build. Eng. 32 (2020). https://doi.org/https://doi.org/10.1016/j.jobe.2020.101494.
[27] O. H.Wallevik, D. Feys, J.E. Wallevik, K.H. Khayat, Avoiding inaccurate interpretations of rheological measurements for cement-based materials, Cem. Concr. Res. 78 (2015) 100–109. https://doi.org/https://doi.org/10.1016/j.cemconres.2015.05.003.
[28] D. Feys, K.H. Khayat, Particle migration during concrete rheometry: How bad is it?, Mater. Struct. 50 (2017). https://doi.org/https://doi.org/10.1617/s11527-016-0992-4.
[29] J. Mewis, N.J. Wagner, Colloidal Suspension Rheology, Cambridge University Press, Cambridge, 2011.
[30] B. Panda, M.J. Tan, Experimental study on mix proportion and fresh properties of fly ash based geopolymer for 3D concrete printing, Ceram. Int. 44 (2018) 10258–10265. https://doi.org/10.1016/J.CERAMINT.2018.03.031.
[31] N. Roussel, Understanding the Rheology of Concrete, Woodhead Publishing Limited, 2012.
[32] M.A. Moeini, M. Hosseinpoor, A. Yahia, Yield stress of fine cement-based mortars: Challenges and potentials with rotational and compressional testing methods, Constr. Build. Mater. 314 (2022).
[33] A. Schwartzentruber, C. Catherine, Method of Concrete Equivalent Mortar—A Novel Tool to Help in Formulation of Concrete with Admixtures, Mater. Struct. 33 (2000) 475–482.
[34] K.H. Khayat, S.-D. Hwang, Effect of High-Range Water- Reducing Admixture Type on Performance of Self-Consolidating Concrete, in: Eighth CANMET/ACI Int. Conf. Superplast. Other Chem. Admixtures Concr., American Concrete Institute, Farmington Hills, MI, 2006: pp. 185–200.
[35] J.J. Assaad, J. Harb, E. Chakar, Relationships between Key ASTM Test Methods Determined on Concrete and Concrete-Equivalent-Mortar Mixtures, J. ASTM Int. 6 (2008).
[36] T.K. Erdem, K.H. Khayat, A. Yahia, Correlating Rheology of Self-Consolidating Concrete to Corresponding Concrete-Equivalent Mortar, ACI Mater. J. (2009).
[37] D. Kabagire, P. Diederich, A. Yahia, New insight into the equivalent concrete mortar approach for self-consolidating concrete, J. Sustain. Cem. Mater. 4 (2015) 215–224. https://doi.org/10.1080/21650373.2015.1018983.
[38] J.H. Lee, J.H. Kim, J.Y. Yoon, Prediction of the yield stress of concrete considering the thickness of

excess paste layer, Constr. Build. Mater. 173 (2018) 411–418. https://doi.org/10.1016/j.conbuildmat.2018.03.124.
[39] M. Hosseinpoor, B.I. Ouro Koura, A. Yahia, E.H. Kadri, Diphasic investigation of the visco-elastoplastic characteristics of highly flowable fine mortars, Constr. Build. Mater. 270 (2021) 121425. https://doi.org/10.1016/J.CONBUILDMAT.2020.121425.
[40] ASTM C305-20, Standard Practice for Mechanical Mixing of Hydraulic Cement Pastes and Mortars of Plastic Consistency, ASTM Int. (2020) 1–3. https://doi.org/10.1520/C0305-20.2.
[41] N. Roussel, C. Stefani, R. Leroy, From mini-cone test to Abrams cone test: Measurement of cement-based materials yield stress using slump tests, Cem. Concr. Res. 35 (2005) 817–822. https://doi.org/10.1016/j.cemconres.2004.07.032.
[42] EFNARC, Specification and Guidelines for Self-Compacting Concrete, (2002).
[43] BS EN 445, Grout for prestressing tendons. Test methods, 2007.
[44] H. Okamura, M. Ouchi, Self-Compacting Concrete, J. Adv. Concr. Technol. 1 (2003) 5–15.
[45] ASTM D4318 – 17, Standard Test Methods for Liquid Limit, Plastic Limit, and Plasticity Index of Soils, ASTM Stand. (2017).
[46] Y.A. Abebe, L. Lohaus, Rheological characterization of the structural breakdown process to analyze the stability of flowable mortars under vibration, Constr. Build. Mater. 131 (2017) 517–525. https://doi.org/10.1016/J.CONBUILDMAT.2016.11.102.
[47] R.S. Ahari, T.K. Erdem, K. Ramyar, Thixotropy and structural breakdown properties of self consolidating concrete containing various supplementary cementitious materials, Cem. Concr. Compos. 59 (2015) 26–37. https://doi.org/10.1016/J.CEMCONCOMP.2015.03.009.
[48] H.A. Barnes, Thixotropy—a review, J. Nonnewton. Fluid Mech. 70 (1997) 1–33. https://doi.org/10.1016/S0377-0257(97)00004-9.
[49] J.J. Assaad, K.H. Khayat, H.A. Mesbah, Assessment of Thixotropy of Flowable and Self-Consolidating Concrete, Aci Mater. J. 100 (2003) 99–107.
[50] K.H. Khayat, J.J. Assaad, Effect of w/cm and high-range water-reducing admixture on formwork pressure and thixotropy of self-consolidating concrete, ACI Mater. J. 103 (2006) 186 – 193.
[51] S. Kawashima, P. Hou, D.J. Corr, S.P. Shah, Modification of cement-based materials with nanoparticles, Cem. Concr. Compos. 36 (2013) 8–15. https://doi.org/10.1016/J.CEMCONCOMP.2012.06.012.
[52] N. Roussel, P. Coussot, “Fifty-cent rheometer” for yield stress measurements: From slump to spreading flow, J. Rheol. (N. Y. N. Y). 49 (2005) 705–718. https://doi.org/https://doi.org/10.1122/1.1879041.

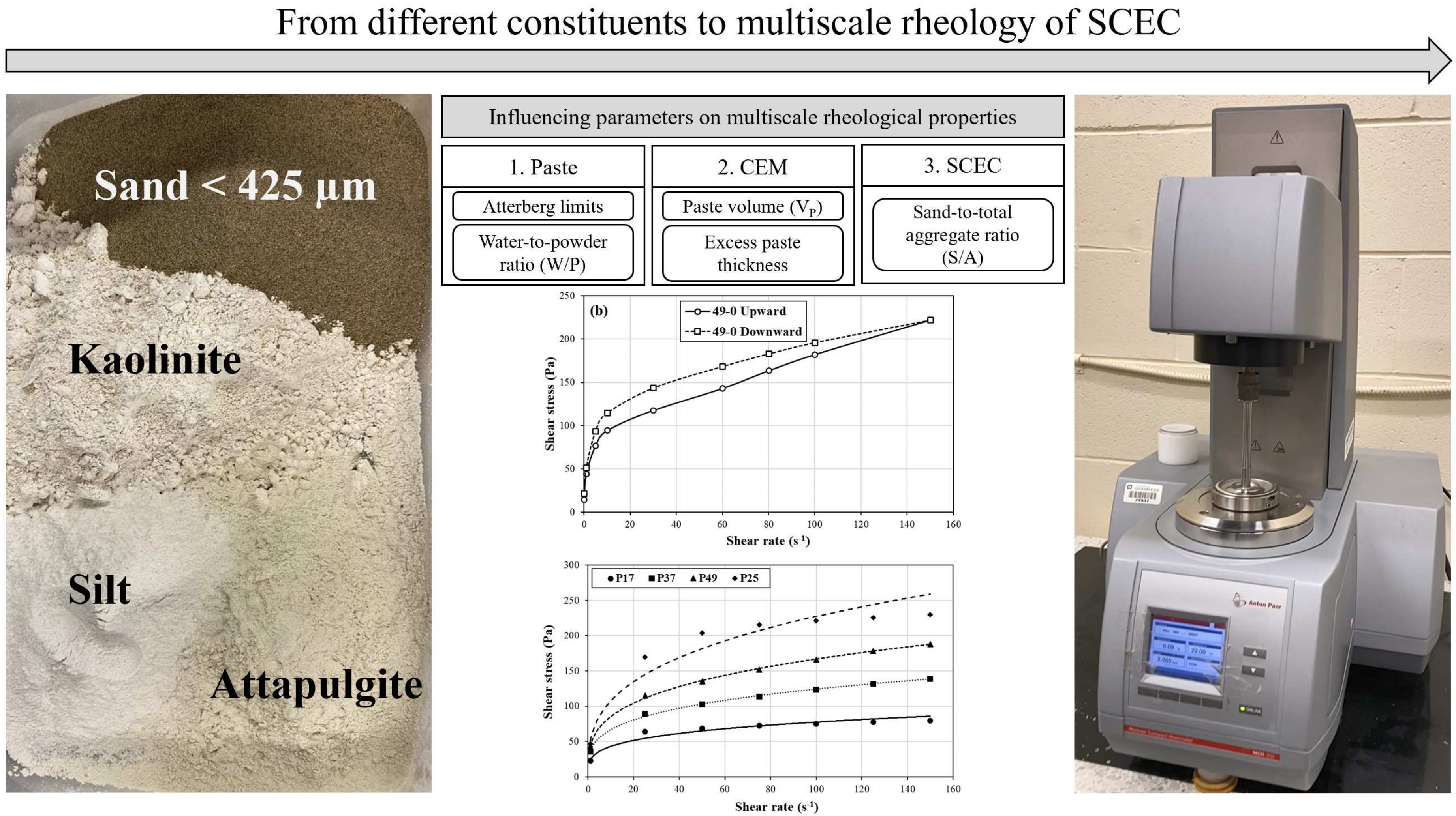

From different constituents to multiscale rheology of SCEC
Sand < 425 μm
Kaolinite
Silt
Attapulgite
Influencing parameters on multiscale rheological properties
1. Paste
Atterberg limits
Water-to-powder ratio (W/P)
2. CEM
Paste volume (V_P)
Excess paste thickness
3. SCEC
Sand-to-total aggregate ratio (S/A)
(b)
49-0 Upward
49-0 Downward
Shear stress (Pa)
Shear rate (s^{-1})
P17 P37 P49 P25
Shear stress (Pa)
Shear rate (s^{-1})
Anton Paar